Washington Public Power Supply System
A JOINT OPERATING AGENCY

P. O. Box 968   3000 Geo. Washington Way   Richland, Washington 99352   Phone (509) 946-9681

Docket 50-397

February 11, 1975
G02-75-37

Mr. A. Giambusso, Director
Division of Reactor Licensing
Office of Nuclear Reactor Regulation
U. S. Nuclear Regulatory Commission
Washington, D.C. 20555

Subject: WPPSS NUCLEAR PROJECT NO. 2
RESPONSE TO QUESTIONS
SACRIFICIAL SHIELD WALL DESIGN

Reference: Letter, W.R. Butler to J.J. Stein, transmitting Request for Additional Information dated July 8, 1974. (GI2-74-11)

Dear Mr. Giambusso:

The attachment provides information requested in the referenced letter. This information includes results of pressure response analyses and structural information for the Sacrificial Shield Wall base design but does not include design information about the Sacrificial Shield Wall itself. We are supplying the information in two parts in order that our Contractors may proceed without delay with the completion of the upper pedestal and wetwell-drywell floor construction. The remaining information will be provided May 15, 1975, so that the Sacrificial Shield Wall itself may be constructed according to schedule.

As discussed with your Dr. John Orndorf, WPPSS is requesting an expedited NRC review of the attached report. In order that we may quickly eliminate any concerns the Staff may have on our responses, WPPSS will be contacting you regarding a meeting to explain this report and resolve any of your concerns.

Forty (40) copies of the attachment are being submitted for your review.

Very truly yours,

J. J. STEIN
Managing Director

JJS:GLG:am

Attachment

1710

cc: JJ Byrnes - Burns and Roe, Inc.
BW Kennedy - Bonneville Power Administration
JJ Verderber - Burns and Roe, Inc.

Subject: WPPSS NUCLEAR PROJECT NO. 2
RESPONSE TO QUESTIONS
SACRIFICIAL SHIELD WALL DESIGN

STATE OF WASHINGTON)
) ss
COUNTY OF BENTON)

Ltr to A. Giambusso, Director, Div. of Reactor Licensing from JJ Stein, Managing Director-WPPSS

J. J. STEIN, Being first duly sworn, deposes and says: That he is the Managing Director of the WASHINGTON PUBLIC POWER SUPPLY SYSTEM, the applicant herein; that he is authorized to submit the foregoing on behalf of said applicant; that he has read the foregoing and knows the contents thereof; and believes the same to be true to the best of his knowledge.

DATED February 11, 1975

J. J. Stein

J. J. STEIN

On this day personally appeared before me J. J. Stein to me known to be the individual who executed the foregoing instrument and acknowledged that he signed the same as his free act and deed for the uses and purposes therein mentioned.

GIVEN under my hand and seal this 11th day of February 1975.

Reba B. Helgeson

Notary Public in and for the State of Washington 510 Sanford
Residing at Richland

SACRIFICIAL SHIELD WALL DESIGN SUPPLEMENTAL INFORMATION

WPPSS 74-2-R2-A

TABLE OF CONTENTS

PREFACE

This report, WPPSS-74-2-R2-A, is the first of two supplemental reports that are planned in response to questions transmitted in the letter from W.R. Butler (AEC) to J.J. Stein (WPPSS) dated July 8, 1974. Two supplemental reports are planned in order to promptly resolve questions most directly affecting construction progress.

The first of these supplements covers the design of the sacrificial shield wall to reactor pedestal connection, the reactor pressure vessel skirt to pedestal connection, and the upper portion of the reactor pedestal. In support of this design, the report describes a transient pressure analysis and a shield wall door design for limiting the pressurization of the shield wall to reactor vessel annulus. The objective of this supplement is to resolve all questions with respect to the design of the upper portion of the pedestal in order that construction of the pedestal may proceed.

The second supplemental report is intended to cover those questions pertaining to the design of the sacrificial shield wall above the connection to the reactor pedestal.

Organization of this report is as shown in the Table of Contents and generally follows the order of questions transmitted by the letter of July 8, 1974.

CONTAINMENT SYSTEMS BRANCH QUESTIONS

QUESTION 1a:

Provide the name and description of the blowdown and pressure transient codes used in the analysis.

ANSWER:

General ELectric Licensing Topical Report NEDO-10320 describes the model used to determine the blowdown flow rates and pressure transients necessary for sacrificial shield wall loading calculations. The blowdown model is based on F.J. Moody's "Maximum Flow Rate of a Single Component, Two-Phase Mixture", Transactions of the ASME, Volume 87, Series C, 1965.

The computer program used for subcompartment pressure analysis is called PEAK. In this program, each compartment may be represented by a single node. Alternatively, a compartment may be divided into several nodes or a single node may be used to represent several compartments, depending on compartment geometry, modelling assumptions and the accuracy desired.

In each node, the volume can be occupied by a two-component, two phase mixture consisting of air and water. Air properties are evaluated on the basis of perfect gas laws. Steam and water properties are evaluated from equations corresponding to the ASME 1967 Steam Tables.(1) Each component and phase is at the same temperature and is uniformly distributed within each node.

Calculations are begun by computing the initial steady-state conditions in each node. Subsequent calculations are performed by using iterative methods to solve the mass and energy balance equations at incremental time steps. In these equations, blowdown mass and energy are introduced into the appropriate nodes at each time step. Mass and energy transfer between any pair of nodes is possible if an opening area is specified between the two nodes. In addition, such transfers may take place between the vapor and liquid phases if condensation or boiloff occur.

The mass balance equations for the i th node for the various phases and components are:

AIR

$$\frac{dM_{Ai}(t)}{dt} = f_{Ai}B_A(t) - \sum_{j=1}^{N} C_{ij}A_{ij}G_{Aij}(t) \quad (1)$$

VAPOR

$$\frac{dM_{Vi}(t)}{dt} = f_{Vi}B_V(t) - \sum_{j=1}^{N} C_{ij}A_{ij}G_{Vij}(t) + R_{Bi}(t) - R_{Ci}(t) \quad (2)$$

LIQUID

$$\frac{dM_{Li}(t)}{dt} = f_{Li}B_L(t) - \sum_{j=1}^{N} C_{ij}A_{ij}G_{Lij}(t) - R_{Bi}(t) + R_{Ci}(t) \quad (3)$$

Where, M_{Ai} = mass of air in node i, lbs

M_{Vi} = mass of vapor in node i, lbs

M_{Li} = mass of liquid in node i, lbs

t = time in seconds

B_A = blowdown rate of air, lbs/sec

B_V = blowdown rate of vapor, lbs/sec

B_L = blowdown rate of liquid, lbs/sec

f_{Ai} = fraction of air blowdown into node i

f_{Vi} = fraction of vapor blowdown into node i

f_{Li} = fraction of liquid blowdown into node i

C_{ij} = flow coefficient between nodes i and j

A_{ij} = flow area between nodes i and j, sq. ft.

G_{Aij} = mass flow rate of air per unit area between nodes i and j, lbs/sq. ft/sec.

G_{Vij} = mass flow rate of vapor per unit area between nodes i and j, lbs/sq. ft/sec.

G_{Lij} = mass flow rate of liquid per unit area between nodes i and j, lbs/sq. ft/sec.

R_{Bi} = rate of boiloff in node i, lbs/sec

R_{Ci} = rate of condensation in node i, lbs/sec

R_{Bi} and R_{Ci} are determined from the thermodynamic condition in the ith node.

The corresponding energy balance equation for the ith node is:

$$\frac{dU_i}{dt} = \frac{d(M_{Ai}u_{Ai})}{dt} + \frac{d(M_{Vi}u_{Vi})}{dt} + \frac{d(M_{Li}u_{Li})}{dt}$$

$$= f_{Ai}B_A h_{BA} + f_{Vi}B_V h_{BV} + f_{Li}B_L h_{BL} \qquad (4)$$

$$- \sum_{j=1}^{N} C_{ij}A_{ij}(G_{Aij}h_{Aij} + G_{Vij}h_{Vij} + G_{Lij}h_{Lij})$$

In this equation, the terms not already defined in the mass balance equation are:

U_i = total internal energy in node i, Btu

u_{Ai} = internal energy of air in node i, Btu/lb

u_{Vi} = internal energy of vapor in node i, Btu/lb

u_{Li} = internal energy of liquid in node i, Btu/lb

h_{BA} = enthalpy of air blowdown, Btu/lb

h_{BV} = enthalpy of vapor blowdown, Btu/lb

h_{BL} = enthalpy of liquid blowdown, Btu/lb

h_{Aij} = enthalpy of air transferred between nodes i and j, Btu/lb

h_{Vij} = enthalpy of vapor transferred between nodes i and j, Btu/lb

h_{Lij} = enthalpy of liquid transferred between nodes i and j, Btu/lb

Blowdown mass and energy are input to the program as functions of time. As indicated by the above equations, blowdown may be directed into any of the nodes or divided among them in a predetermined fashion. In this report, the doors discussed in Question 2a split the blowdown between (1) the drywell and (2) the annulus between the reactor vessel and the sacrificial shield wall. The blowdown term is included in all equations for completeness. In most cases, it does not exist and can be set equal to zero.

Mass and energy transfer among the nodes is computed on the basis of pressure differences, after first determining if the flow is critical or subcritical. Flow is critical if:

$$\frac{P_j}{P_i} \leq \left(\frac{2}{1+\gamma}\right)^{\frac{\gamma}{\gamma - 1}} \qquad (5)$$

In this equation,

P_i = absolute pressure in node i, lb/sq. ft.

P_j = absolute pressure in node j, lb/sq. ft.

γ = specific heat ratio, c_p/c_v

For the sub-critical case, the mass flow rate per unit area is determined from the equation:

$$G_{ij} = \sqrt{\frac{2g\gamma}{\gamma - 1} P_i \rho_i \left[\left(\frac{P_j}{P_i}\right)^{\frac{2}{\gamma}} - \left(\frac{P_j}{P_i}\right)^{\frac{\gamma+1}{\gamma}}\right]} \qquad (6)$$

For critical flow, the mass flow rate per unit area is determined from the equation:

$$G_{ij} = \sqrt{\frac{2g\gamma}{\gamma - 1} \; P_i \, \rho_i \left[\left(\frac{2}{\gamma + 1}\right)^{\frac{2}{\gamma - 1}} - \left(\frac{2}{\gamma + 1}\right)^{\frac{\gamma + 1}{\gamma - 1}} \right]} \qquad (7)$$

In these equations the nomenclature is the same as above except for the additional items noted below:

G_{ij} = total flow rate per unit area between nodes i and j, lbs/sq. ft/sec.

g = acceleration of gravity, ft/sec^2.

ρ_i = fluid density in node i, lbs/cu. ft.

In the above equations the specific heat ratio, γ, is first determined for the mixture of vapor and entrained liquid water as indicated by Figure 11 of the ASME 1967 Steam Tables.[2] The average specific heat ratio is then obtained by weighting this value with that of the air in the mixture.

The flow coefficient in the mass and energy balance equations, above, is computed from the equation:

$$C_{ij} = \sqrt{\frac{1}{1 + (K_{cont} + K_{fric} + K_{exp})}} \qquad (8)$$

where, K_{cont} = contraction loss coefficient

K_{fric} = friction loss coefficient

K_{exp} = expansion loss coefficient

The flow coefficients depend on the configuration of the flow path between the pair of nodes under consideration. Physically, the K values represent the head loss expressed as velocity heads. The values of K_{cont} and K_{exp} are determined from the Crane Co. Handbook.[3] K_{fric} is equal to fL/D, where f is the friction factor,[3,4] L is the length of the flow path and D is the hydraulic diameter of the flow path.

QUESTION 1b:

Justify the blowdown model used showing that it adequately represents the short-term mass and energy release rates.

ANSWER:

Section 2 of NEDO-10320 compares blowdown rates calculated from the Bodega Bay and Humbolt Bay pressure suppression tests with those predicted by the Moody model. These comparisons show good agreement, and confirm that the Moody model is increasingly conservative as the break size is increased.

QUESTION 1c:

Provide and justify, preferably by comparison with experimental data, the equations or correlations used to calculate flow between compartments. Include a discussion of the critical flow model and discharge coefficient applied to critical flow.

ANSWER:

Please see the information provided in the answer to Question 1a. In addition, it should be noted that reference 5 has previously submitted the results of calculations using the PEAK program for the 13 benchmark problems for subcompartment analysis issued by the Commission.

QUESTION 1d:

Discuss the method of treating the air-steam-water mixture in subcompartment thermodynamics and fluid mechanics.

ANSWER:

Please see the information provided in the answer to Question 1a.

QUESTION 2a:

Provide a table of the blowdown mass and energy release rates used in the analysis.

ANSWER:

Recirculation line blowdown data:

Time (Sec)	Liquid* Flow (lb/sec)	Vapor Flow (lb/sec)	Liquid Enth (Btu/lb)	Vapor Enth (Btu/lb)
0	25870	0	550.5	1189
8	26560	0	561.7	1186
18.25	26820	0	565.8	1185
18.3	10000	5300	563.2	1186
22.5	6986	4727	538.2	1193
25.1	5481	4145	512.6	1198

*Note:
The data presented here is the same as that presented in the PSAR, page Q. 5.2-1. For the calculations discussed in this report the liquid flow blowdown data was increased by 20% over the values presented here and in the PSAR to account for water inventory in the recirculation line.

Only a portion of the blowdown will enter the annular space between the sacrificial shield wall and the reactor pressure vessel. Figures 1 through 3 illustrate the sacrificial shield wall flow limiting door design concept which results in the majority of the blowdown from the postulated break entering the drywell rather than the annulus. Conceptually, this design is illustrated in Figure 4. The fraction of blowdown which enters the shield wall annulus is based on the resistance to fluid flow through the restricted area of the doors as compared to the resistance to fluid flow toward the drywell. This is calculated as a function of the areas and flow coefficients in each direction away from the break.

For nominal door dimensions, the flow split is 8.6 to 1. The blowdown listed above is split between the drywell and the annulus by this ratio. Results of the pressure loading calculations from this flow split for the 60 node case discussed later in this report are shown in Figures 23 and 24. Also shown in Figures 23 and 24 are results based on a flow split of 7.5 to 1 representing the worst case tolerances for the weir plates (see Figures 1 and 2) which restrict flow into the annulus. Worst case tolerances for the weir plates are those which allow the largest area for flow to the annulus. Nominal and worst case fit-up for the weir plates are illustrated in Figure 5. Results of these two cases will be discussed later in this report.

In order to eliminate possible concern with respect to blockage of the flow path to the drywell following the break, pipe insulation is being left off that portion of piping within the nozzle sleeve and shield doors. The pipe insulation configuration in the vicinity of the shield wall opening is shown in Figure 6. The pipe insulation at the outboard face of the shield wall would be moved to clear the opening in the event of pipe break by the recoil of the broken pipe and by the fluid flow from the break.

QUESTION 2b:

Provide and justify the break type and area used in the analysis.

ANSWER:

A complete circumferential break of the 24 inch recirculation line at the circumferential weld to the reactor vessel nozzle safe end is assumed in the analysis. Sufficient separation of the broken pipe from the reactor vessel nozzle is assumed to allow maximum flow from the broken line.

A longitudinal break is not assumed since the run of pipe within the shield wall opening is a straight run without a significant change in flexibility. The first location with a significant change in flexibility where a longitudinal break would normally be assumed is at the elbow outside the shield wall opening.

Postulating a 24 inch recirculation line break allows the largest fluid mass and energy to be available for pressurization of the annulus between the reactor vessel and the sacrificial shield wall. The elevation of the 24 inch recirculation lines is lower in the shield wall annulus than other high energy lines except the 12 inch recirculation inlets which are at approximately the same elevation. Vent areas which are available to relieve the pressure buildup within the annulus are at or near the top of the shield wall, and therefore postulated line breaks which are at lower elevations will tend to cause more severe pressure differentials. In addition, a high pressure differential at a lower elevation in the annulus will transmit a larger shear force to the base connection of the shield wall than the same pressure differential applied at a higher elevation.

The discussion above does not obviate the need to investigate other high energy lines which pass through the shield wall. Each of these lines is being investigated either to establish that a flow limiting door design is unnecessary or to establish a door design which will limit the loading on the shield wall base connection to something less than is obtained from the recirculation line break. Each of these openings in the shield wall is amenable to a door design similar to the design for the recirculation lines if calculations determine that such a design is necessary.

QUESTION 2c:

Provide sufficiently detailed drawings showing the arrangement of the reactor vessel, sacrificial shield, insulation, and recirculation line from which subcompartment volumes and vent areas can be determined.

ANSWER:

Volumes and vent areas can be determined from Figures 7 through 9 and the nozzle sizes given in Figure 10. The information given below describes the method used to establish volumes and vent areas for the calculations described in this report.

The calculations performed first considered that all the blowdown to the annulus entered the space between the RPV insulation and the RPV. Throughout the transient the insulation was assumed to stay in place rather than being moved against the shield wall. This assumption conservatively limits the volume between the insulation and RPV to the volume that would exist initially. Vent area is available in this case through the stabilizer region at the top of the annulus and out to the drywell through blowoff panels in the insulation above the stabilizers. Pressure may also be relieved through the blowoff panel illustrated in Figure 8, and up the outside of the insulation to the vent area at the top of the annulus. This case caused lower differential pressures across the annulus than the following case which will be described in more detail.

The second set of calculations assumed that all the blowdown to the annulus entered the space between the RPV insulation and the shield wall. Again, the insulation was conservatively assumed to stay in place rather than collapsing against the RPV and thereby increasing volumes. The only vent areas that were assumed were those through the stabilizer region at the top of the annulus and through shield wall openings A-3A through A-3F and A-4A and A-4B (See Figure 7). These shield wall openings are clear openings without shielding doors. Vent areas were determined by subtracting the area occupied by the piping and pipe insulation from the total area of the opening. See Figure 10 for the piping passing through various shield wall openings.

Additional, but smaller, vent areas around piping which passes through shield wall openings with shield doors were neglected. Vent areas through openings A-21A and A-21B, both of which do not have shielding doors, were neglected due to lack of symmetry. Computer models use a 180° arc of the shield wall requiring symmetry for vent areas in the shield wall in order to credit vent areas correctly. Possible vent areas available into ventilation ducts A-26A through A-26C and A-12A through A-12E were neglected. Vent area through opening A-6 near the top of the wall was neglected. Inspection doors A-9A and A-9B were conservatively assumed to remain closed.

QUESTION 2d:

Describe the nodalization sensitivity studies performed to determine the minimum number of volume nodes required to conservatively predict the maximum pressure for the sacrificial shield annulus. These studies should include consideration of spatial pressure variations; i.e., pressure variations circumferentially, axially and radially within the annulus.

ANSWER:

A 180° arc of the sacrificial shield wall to reactor pressure vessel annulus was used for studies of pressure within the annulus in order to take advantage of the symmetry of the annulus. The annulus was divided at the vertical centerline of the postulated pipe break. One half of the blowdown into the annulus was introduced into this 180° portion of the annulus.

Figures 11 and 12 illustrate nodal volumes. The 17 nodes shown for this 180° arc correspond to a 34 node analysis of the complete annulus. Vent areas were taken as indicated in the response to Question 2c (through the stabilizer region and through openings A-3A through A-3F and A-4A and A-4B). Results of calculations for this 17 node case are given in Figure 13. Figure 13 shows the pressures in each node at the time of maximum shear force and moment at the base of the annulus.

Figure 14 shows results for a 50 node case (25 nodes per 180° of annulus). The volume of nodes close to the break has been made smaller since the pressure gradient will be greater close to the break node. As expected, this node arrangement therefore gives a higher calculated maximum shear force and moment than the previous case. The results are compared in Figures 23 and 24.

Figures 23 and 24 are graphs of shear force and moment at the base of the shield wall as a function of time. These graphs have been prepared by calculating the shear force and moment at different time steps from the results of the PEAK computer program. These graphs indicate that the maximum shear and moment occur between .03 and .04 seconds with the time of the peak varying slightly depending upon the number of nodes used in the PEAK program.

Figure 15 shows results for a 60 node case (30 nodes per 180° of annulus). Volumes of nodes closest to the break have been made smaller. A comparison of results is given in Figures 23 and 24. As is shown in Figures 23 and 24 the increases in shear force and moment is about 2% over the 50 node case.

This case and the previous two cases have been used to establish a conservative value of shield wall base shear and moment as a result of pressure within the annulus as shown in Figures 23 and 24. In the structural design, this value based on annulus pressure was multiplied by a dynamic impact factor (1.7) and combined with other loadings (discussed in Structural Engineering Branch Question 2 which follows) to establish the structural design.

QUESTION 2e:

Provide a schematic flow diagram showing the nodalization of the shield annulus and specifying nodal net free volumes and interconnecting flow path areas.

ANSWER:

Schematic flow diagrams for the 3 cases discussed in Question 2d are given in Figures 16, 17, and 18. Flow coefficients are also shown for vent areas.

QUESTION 2f:

Provide and justify values of vent loss coefficients and/or friction factors used to calculate flow between nodal volumes. When a loss coefficient consists of more than one component (e.g., entrance loss, exit loss) identify each component and its value.

ANSWER:

Flow coefficients between nodal volume are shown in the schematic flow diagrams, Figures 16, 17, and 18. The equation used to establish the flow coefficient between nodal volumes is discussed in the response to question 1a (See equation 8).

Within the annulus, for example between node 8 and node 9, the friction loss coefficient is used to establish the flow coefficient since no contraction or expansion loss occurs. The friction loss coefficient is determined from reference 3 based on the hydraulic diameter between nodes and the path length from the center of one node to the center of the adjacent node.

From the annulus to the drywell (e.g., node 18 to node 30 in the 60 node case) the flow coefficient will consist of three terms - an expansion loss coefficient, a contraction loss coefficient, and a friction loss coefficient. The expansion loss coefficient and the contraction loss coefficient are conservatively taken as 1.0 and 0.5 respectively as given in reference 3. The friction loss coefficient is determined from reference 3 based on the hydraulic diameter of the node in the annulus (e.g. node 18) and the path length from the center of the node in the annulus (e.g. node 18) to the drywell.

For flow across elevation 527' (e.g., node 22 to node 27 in the 60 node case), the flow coefficient will consist of two terms - an expansion loss coefficient and a friction loss coefficient. The expansion loss coefficient is a function of the hydraulic diameters as given in reference 3 for a sudden enlargement. The friction loss coefficient is determined from reference 3.

QUESTION 2g:

Discuss the manner in which movable obstructions to vent flow (such as insulation, ducting, plugs and seals) were treated. Include analytical justification if credit is taken for the removal of such items to obtain vent area. Justify your assumption that vent areas will not be more than 50% plugged by insulation or other displaced objects.

ANSWER:

Two cases which were studied are discussed in the answer to Question 2c. In the first case all the blowdown to the annulus was assumed to enter the space between the RPV insulation and the RPV. Lateral vent area through the RPV insulation to the annulus on the outside of the RPV insulation was considered to be completely blocked. Movement or separation of the sections of insulation was not assumed. This assumption is conservative since the volume available for blowdown is limited to the volume of the annulus on the inside of the insulation, and vent areas through the openings in the shield wall and through the stabilizer region outside the insulation through separated pieces of insulation were not considered available.

The second case, which resulted in the highest differential pressures across the annulus, assumed that all the blowdown to the annulus entered the space between the RPV insulation and shield wall. Lateral vent area through the RPV insulation to the annulus on the inside of the RPV insulation was considered to be completely blocked. Movement toward the RPV or separation of the insulation was not assumed. This assumption is conservative since the volume available for blowdown is limited to the small volume of the annulus outside of the insulation and vent areas through the stabilizer region inside the insulation were not considered available. The conservatism of this assumption is apparent from the resulting distribution of pressure which would tend to move the RPV insulation toward the RPV-increasing the volume available for blowdown and increasing the vent area through the stabilizer region.

The percent (50%) of vent area plugged by insulation which was discussed in WPPSS-74-2-R2 is not applicable to the new analysis described in this report. Rather than use the entire volume of the annulus between the shield wall and the RPV and assume a certain percentage of the total vent area blocked, this analysis has conservatively used the limited volumes on either side of the insulation in each case for the initial blowdown and the related limited vent areas discussed above and in response to Question 2c.

QUESTION 2h:

Provide a curve of shield differential pressure as a function of time indicating spatial response where appropriate.

ANSWER:

Figures 19 through 22 are curves of shield differential pressure as a function of time between the most relevant nodes affecting shield wall shear force and moment. It is of interest to note by comparison with Figures 24 and 25 that the maximum total shear force and moment on the structures at the base of the sacrificial shield wall do not occur at the time of the maximum differential pressure at the elevation of the break. Instead, the shear and moment continue to increase for a short time after this peak differential pressure is reached at the break elevation.

QUESTION 2i:

Specify the design differential pressure of the sacrificial shield wall.

ANSWER:

Figures 23 and 24 illustrate the design basis for the differential pressure across the shield wall annulus. The design basis is defined in terms of shear and moment at the base of the wall rather than in terms of a particular pressure. Since the pressure varies with position, specifying a particular design basis pressure would not be meaningful. Figures 13, 14, and 15 illustrate pressures in each node at the maximum values of shear force, and moment for the 34, 50 and 60 node cases, respectively.

STRUCTURAL ENGINEERING BRANCH QUESTIONS

QUESTION 1:

Provide a statement that the design criteria and the design methods for the sacrificial shield are in accordance with Document (B) cited above.

ANSWER:

The design criteria and the design methods for the structures which are the subject of this supplemental report, i.e., the connection between the shield wall and the pedestal, the connection between the RPV skirt and the pedestal, and the upper portion of the pedestal are in accordance with Document (B), Structural Engineering Branch Directorate of Licensing - Structural Design Criteria For Evaluating The Effects Of High-Energy Pipe Breaks On Category I Structures Outside The Containment.

QUESTION 2:

Furnish the applicable information listed in the Standard Format in sections cited above (3.5, 3.7, 3.8.3, 3.8.4, and 3.8.5).

ANSWER:

The information discussed in this supplemental report pertains to the connection between the shield wall and the pedestal, the connection between the RPV skirt and the pedestal, and the upper portion of the pedestal. The report therefore deals primarily with section 3.8.3, Concrete and Steel Internal Structures of Steel or Concrete Containment, of the Standard Format and Content of Safety Analysis Reports (Rev. 1).

The subject matter of Sections 3.8.4, Other Seismic Category I Structures, and 3.8.5, Foundations, is not applicable to this report. These two sections cover information on foundations and other structures which do not control the design of structures discussed in this report under section 3.8.3. Section 3.5, of the Standard Format covers missile protection measures and provisions incorporated in plant design. Missiles which might be generated from the shield wall and missiles which might strike the shield wall will be discussed in the second supplemental report to be prepared on the shield wall. Loads due to missiles generated elsewhere within the containment would be small in comparison to the combinations of loadings covered in this report, e.g., differential pressure loading, earthquake loading, etc., and therefore do not control the design of the base connections of the shield wall and RPV. Section 3.7 of the Standard Format covers analytical methods and procedures used to establish the seismic loadings on structures. These methods are discussed in Chapter 12 of the PSAR. The design of the base connections conform to the seismic loading adopted for this project. Seismic loading, together with other loads in the combinations listed in Document (B), is discussed in the paragraphs which follow.

The following information is organized to follow the outline presented in section 3.8.3 of the Standard Format as issued by Regulatory Guide 1.70.9, November, 1974.

3.8.3 CONCRETE AND STEEL INTERNAL STRUCTURES OF STEEL OR CONCRETE CONTAINMENTS

The structures internal to the containment which are discussed herein are the base connections of the SSW and the RPV to the pedestal and the upper portion of the pedestal.

3.8.3.1 Description of the Internal Structures

Details of the base connections and upper pedestal are shown in Figures 25, 26, and 27. These figures comprise a plan at the top of the pedestal of base details of the SSW and RPV and sections illustrating such details.

The following describes the SSW base and the upper portion of the pedestal.

a. The SSW base is permitted to grow radially with respect to the bearing plate which, in turn, is anchored to the pedestal. Towards this end, the anchor bolt holes and the shear lug radial slots in the SSW base plate are provided with extra clearance in the radial direction.

b. Shear lugs welded to the SSW bearing plate and passing through the radial slots in the SSW base plate will transmit shear in the tangential direction from the base plate to the bearing plate. Differential displacement in the radial direction between base plate and bearing plate, caused primarily by thermal growth, can take place practically unrestrained.

c. Transmission of tangential shear from the bearing plate into the concrete pedestal will be by 7/8" x 8" headed stud shear connectors welded to the underside of the bearing plate. The connectors are arranged in rows of 8 each with a row spacing of 7.5 degrees circumferentially.

d. The bearing plate will not be in position during construction of the upper portion of the pedestal. To accommodate the bearing plate studs, pockets will be provided in the top of the pedestal. These will be filled with grout at the time of installation of the bearing plate.

e. Anchor bolts connect the SSW base plate to the concrete pedestal. These bolts provide the necessary resistance to uplift forces caused by postulated seismic and pipe rupture events. In addition, they serve as the required shear friction reinforcement for transmission of the tangential shear into the upper portion of the pedestal. Groups of four 2½ inch diameter anchor bolts are spaced at 15° circumferentially.

The following describes the RPV base and the upper portion of the pedestal:

a. The RPV skirt flange is fixed in position to the pedestal by the anchor bolts. Two 3 inch diameter bolts are provided at 6° spacing.

b. Tangential shear from the RPV skirt flange is transmitted to the bearing plate below via the above anchor bolts.

c. The tangential shear is transmitted by the bearing plate into the concrete pedestal by means of 7/8" x 8" headed stud shear connectors welded to the underside of the bearing plate. The connectors are arranged in rows of 5 each with a circumferential row spacing of 6 degrees.

d. Pockets are provided in the top of the pedestal during pedestal construction. The bearing plate studs will be grouted into these pockets at the time of bearing plate installation.

e. The anchor bolts which connect the RPV skirt flange to the concrete pedestal provide the necessary resistance to uplift forces due to postulated seismic and pipe rupture events. In addition they serve as the required shear friction reinforcement for transmission of the tangential shear into the upper portion of the pedestal.

3.8.3.2 Applicable Codes, Standards, and Specifications

The following codes are applicable:

a. American Institute of Steel Construction (AISC) Specification for the Design, Fabrication and Erection of Structural Steel for Buildings, 1969.

b. American Concrete Institute (ACI), Building Code Requirements for Reinforced Concrete ACI 318-71.

3.8.3.3 Loads and Load Combinations

The loads listed below are applicable to the structures involved and were considered in the combinations specified hereinafter for the design of these structures.

a. Dead loads, live loads, and thermal loads due to operating conditions

b. Operating Basis Earthquake

c. Safe Shutdown Earthquake

d. Loads due to high energy pipe ruptures

Based on a review of the magnitude of the above loads, it is ascertained that of the load combinations defined in Document B, only those listed below control the design (In the following, the terminology and paragraph numbering of Document B is used for cross reference purposes). These combinations, using the terminology of Document B, are listed below.

For steel structures, i.e., the SSW and RPV base connections:

D.1 (b) (1) $0.90Y = D + L + Ta + Ra + 1.5Pa$

(2) $0.90Y = D + L + Ta + Ra + 1.25Pa + 1.0\ (Yj + Yr + Ym) + 1.25\ Feqo.$

(3) $0.90Y = D + L + Ta + Ra + 1.0Pa + 1.0\ (Yj + Yr + Ym) + 1.0\ Feqs.$

For concrete structures, i.e., the pedestal:

C.1 (1) U = D + L + Ta + Ra + 1.5Pa

(2) U = D + L + Ta + Ra + 1.25Pa

+ 1.0 (Yj + Yr + Ym) + 1.25 Feqo.

(3) U = D + L + Ta + Ra + 1.0Pa

+ 1.0 (Yj + Yr + Ym) + 1.0 Feqs.

The concrete design complies with the Strength Design Method of the ACI Building Code (ACI 318-71). The steel design complies with the 1969 AISC Specification for the Design, Fabrication, and Erection of Structural Steel for Buildings, with allowable stresses of 0.90 of yield. For loading combinations including pipe break effects, the plastic section modulus of steel shapes was used in computing the required section strength.

3.8.3.4 Design and Analysis Procedures

Design and analysis procedures applicable to the structures in this report are described below.

a. Effect of Loads Acting on the SSW and RPV at the Pedestal Interface.

(1) Seismic Loads - The effect of horizontal seismic loads is defined at the interface in terms of the overall base shear and the overall overturning moment. The base shear and overturning moment are obtained from a dynamic analysis of a discrete mathematical idealization of the entire reactor building structure. The vertical forces on the interface due to seismic events are also obtained from dynamic analysis.

(2) Loads Due to Pipe Breaks (pressure, pipe reactions, etc.) - The effects of these loads is also defined in terms of the base shear and overturning moment at the interface. Towards this end, both the SSW and the RPV are assumed to act as elastic beams fixed at the base and simply supported at the level of the stabilizer truss.

(3) Special Pipe Breaks - Certain pipe breaks are found to cause a concentrated vertical reaction over a limited portion of the interface.

b. Distribution of Reactions at Interface due to Base Shear and Overturning Moment

(1) The distributions of shearing force and axial force at the interface are those associated with simple flexural theory.

(2) The shearing force per unit length of arc due to base shear is circumferential in direction and varies sinusoidally in magnitude. Taking the base shear direction at 0^o, the shearing force is maximum at 90^o and 270^o.

(3) Axial force per unit length of arc due to overturning moment varies linearly with the distance from the neutral axis. If the moment direction is taken consistent with shear force direction in (2) above, the maximum axial force occurs at 0^o and 180^o and in general at 90^o from the location of maximum shear force.

c. Controlling Load Combinations

(1) General - Load combinations are investigated separately for each component structure at the interface. For each component, the controlling load combination for the different effects are evaluated as noted below.

(2) SSW Connection - Design considered the following aspects:

(a) Transmission of Shear - Maximum base shear occurs with Load Combination D.1 (b) (2) of Document B, as a result principally, of pipe rupture reaction and annulus pressurization. The mechanism of transfer of shear from the SSW base into the pedestal is described in 3.8.3.1 and is shown in Figures 25 through 27.

In short, shear lugs transfer the shear from base plate to bearing plate and stud shear connectors are used to transfer the shear from the bearing plate to the concrete pedestal. The shear capacity required at the location of maximum unit shear force is furnished around the entire circumference of the SSW base.

(b) Uplift - Maximum tension used for anchor bolt design occurs with the same Load Combination D.1 (b) (2) as in subparagraph (a) above and due to the same loads. The location of maximum unit tension occurs at 45° to the direction of the shear loads. Contributing to the maximum unit tension are the axial forces due to maximum overturning moment, vertical seismic forces, and the shear friction tensile force due to maximum base shear. Four 2½ inch diameter anchor bolts, anchored into the concrete pedestal as shown in the figures, provide the necessary resistance against maximum uplift over a 15° arc. The same capacity is furnished uniformly around the circumference of the SSW base.

(c) Thermal Effects - As noted in 3.8.3.1 in the description of the structures, the SSW base is permitted to grow radially with respect to the bearing plate below which is anchored to the concrete pedestal. With temperature differential, a radial horizontal force between the SSW base and the bearing plate occurs; this force is limited to the frictional force of impending motion. Since the bearing plate is constructed as a continuous ring plate, the radial force is resisted by the bearing plate.

(3) RPV Connection - Design considered the following aspects:

(a) Transmission of Shear - Maximum base shear occurs with Load Combination D.1 (b) (2) of Document B, under the action

of the operating basis earthquake, pipe rupture reaction and annulus pressurization The mechanism of transfer of shear from the RPV skirt flange into the pedestal is described in 3.8.3.1 and is shown in Figures 25 through 27. Shear is transferred from the flange to the bearing plate via the anchor bolts and then from the bearing plate to the concrete pedestal by means of stud shear connectors embedded in the pedestal. The shear capacity required at the location of maximum unit shear force is also provided around the entire RPV base.

(b) Uplift - Maximum tension used for anchor bolt design occurs with the same Load Combination D.1 (b) (2) as in preceding subparagraph (a) and is due to the same loads. The location of maximum unit tension occurs at 45° to the direction of the shear loads. Contributing to the maximum unit tension are the axial forces due to maximum overturning moment, vertical seismic forces, and the shear friction tensile force due to maximum base shear. Two 3 inch anchor bolts anchored into the concrete pedestal provide the necessary resistance against maximum uplift over a 6° arc. The same capacity is furnished uniformly around the circumference of the RPV base.

(c) Thermal Effects - Since the RPV flange is fixed in position by the anchor bolts, temperature differential between the flange and the pedestal results in force transmission. A temperature differential of 40°F has been used in the design of the connection. The resultant radial force is transmitted by shear in the anchor bolts into the RPV bearing plate and from the bearing plate into the pedestal via the stud shear connectors.

(4) Top of Pedestal - Design of the top of the pedestal is based on the simultaneous reactions from the SSW and the RPV. The physical effects noted below are evaluated based on the controlling load combinations:

(a) Bending Moment and Tension - Maximum local moment and tension on the concrete section of unit arc length are evaluated in turn for the case of maximum uplift from the SSW and the case of maximum uplift from the RPV. The case of maximum uplift from the SSW results from Load Combination C.1 (3) and involves vertical pipe rupture load and the Safe Shutdown Earthquake. The case of maximum uplift from the RPV results from Load Combination C.1 (2) and includes loads due to the operating basis earthquake, pipe rupture reaction and annulus pressurization.

(b) Local Bearing - Two cases are involved as in subparagraph (a) preceding. The same Load Combinations are controlling.

(c) Overall Shear on Pedestal - Maximum shearing stresses result from Load Combination C.1 (3) which includes radial pipe rupture loads and the Safe Shutdown Earthquake loading. In this regard it is noted that the annulus pressure loading on the SSW and RPV is not comtrolling since the base shears from these two structures are in opposite directions and tend to cancel.

(d) Overturning Moment on Pedestal - Maximum axial stresses result from the same loading as in (c) preceding, namely Load Combination C.1 (3).

(e) Thermal Effects - The thermal reflective insulation shown in Figure 8 insulates the top of the pedestal. Temperature differential in the upper portion of the pedestal in the radial and vertical direction is therefore limited.

3.8.3.5 Structural Acceptance Criteria

The applicable load combinations are listed under paragraph 3.8.3.3. These load combinations involve loads of the severe environmental, extreme environmental and abnormal categories and are combinations for factored load conditions. The required sectional strength of the concrete pedestal is calculated using the ultimate strength design method of ACI 318-71 with the applicable capacity reduction factor. For the SSW and RPV base connection, the maximum allowable stresses are 90 percent of the yield stresses listed in the 1969 AISC Specification for the Design, Fabrication and Erection of Structural Steel for Buildings.

3.8.3.6 Materials, Quality Control, And Special Construction Techniques

3.8.3.6.1 Structural Steel

Structural steel conforms to ASTM A36, except for the following for which the specification designation is noted:

a. Anchor Bolts

(1) For sacrificial shield wall (SSW) ASTM A 307

(2) For reactor pressure vessel (RPV) ASTM A 307

b. Reactor Pressure Vessel

(1) Skirt flange ASME SA 516 Grade 70

c. Connections For SSW

(1) Shop connections, welded AWS D1.1

(2) Field connections, welded AWS D1.1

d. Connections For RPV

(1) Skirt flange segments, shop welded as an integral part of the RPV in accordance with ASME Code Section III, Class I.

(2) Bearing plate segments, field bolted ASTM A 307

e. Stud Shear Connectors

(1) Stud shear connectors conform to ASTM A 108.

3.8.3.6.2 Concrete

All concrete materials are approved on the basis of conformance to the specifications and standard technical methods of the ASTM, and are from sources determined acceptable prior to start of construction. Concrete is made from suitable aggregates and the concrete properties are determined by laboratory tests. Concrete admixtures are used to minimize the mixing water requirements and increase workability. The specified compression strength at 28 days is:

	Specified Strength (psi)	Required Average Test Strength* (psi)
RPV pedestal and SSW	4000	4550

*ACI-301-72, assuming standard deviation of 300 to 400 psi. Water used in mixing of concrete, mortar, and grout is clean and free from deleterious amounts of silt, oil, acids, alkali, salts, and organic substances. Water with chlorides calculated as Cl, in excess of 1,000 parts per million (ppm), or sulfates, calculated as SO_4, in excess of 1,000 ppm are not permitted.

All concrete work is in accordance with ACI-318-71, "Building Code Requirements for Reinforced Concrete", and applies with the following specifications:

Material	ASTM Specification
Cement Type II, low alkali	C 150
Aggregate	C 33
Natural Cement	C 618, Pozzolan Class N
Air-entraining admixture in RPV pedestal only	C 260

Water-reducing agents in RPV pedestal and SSW	C 494

3.8.3.6.3 Reinforcing Bars

Reinforcing bars are not used in the SSW. Reinforcing bars for the RPV pedestal are deformed bars meeting the requirements of ASTM A 615, Grade 40 for #5 bars and smaller and ASTM A 615, Grade 60 for bars #6 through #18. Placing and splicing of bars is in accordance with the requirements of ACI 318-71. For mechanical (Cadweld) splices for reinforcing bars see 3.8.3.6.7. Milltest results, in accordance with ASTM A 615, are obtained from the reinforcing steel supplier for each heat of steel to substantiate the required compositions, strength, and ductility. Certified reports of chemical and physical tests performed are submitted to the Owner for approval All reports are documented and submitted even though they might indicate a heat that is inadequate. The tests document the yield strength, ultimate strength, percent elongation, and chemical composition. To assure adequate ductility two full size bars of each size from each heat are subjected to 90 degree bend tests using a pin diameter ten times the diameter of the bar being bent. In addition, a full section of bar, as rolled, is tested to substantiate strength and ductility. One test is performed for every 50 tons of reinforcing - or at least one test in each heat. The tension test is made on each bar size in the heat.

3.8.3.6.4 Grout

Grout between the top of the RPV pedestal and the bearing plates for the SSW and the RPV meets the requirements of the following U.S. Corps of Engineers specifications:

CRD-C-558	Specification for Expansive Grouts
CRD-C-589	Methods of Sampling and Testing Expansive Grouts

The specified compressive strength at 28 days is 5000 psi.

3.8.3.6.5 Control Tests for Concrete

The following routine concrete control tests are made on the concrete sampled from the discharge of the mixer. Sampling and testing is performed for each 100 cubic yards of concrete production or fractions thereof.

a. Temperature of concrete for each 50 cubic yards.

b. Slump of concrete (ASTM C 143) for each 50 cubic yards.

c. Air content (ASTM C 173 or C 231) for each 50 cubic yards.

d. Compressive strength of concrete (ASTM C 31 tested in accordance with ASTM C 39). Sufficient 6 x 12 inch concrete cylinders are molded for tests.

3.8.3.6.6 Evaluation of Test Results

Concrete Cylinders - One cylinder from alternate sets is tested at 7 days and one cylinder from every other set is tested at 14 days for information. Two cylinders from each set are tested at 28 days for acceptance and the test result is considered the average of two cylinders tested at 28 days. The fourth cylinder from each set is tested at 90 days for information. Records are maintained in accordance with ACI 214.

Splices of Reinforcement - ACI 318-71 applies to lapped splices for bar sizes 11 and smaller. Normally, bar sizes 14 and larger are spliced by mechanical connectors (Cadwelds). Where space limitations in the upper portion of the pedestal prohibit the use of lap splices for bar sizes 11 and smaller, mechanical Cadweld connectors are used. The mechanical splice will be designed to develop the specified minimum ultimate strength. Reinforcing spliced with mechanical connectors conforms to 3.8.3.6.7.

3.8.3.6.7 Mechanical (Cadweld) Splices for Reinforcing Bars

All splices made by the Cadweld process use clamping devices, sleeves, charges, etc., as specified by the Cadweld Splice Instruction Sheets for B - and T -series connections. C - series materials are not used.

Testing of reinforcing-bar mechanical splices is in accordance with Regulatory Guide 1.10, Mechanical (Cadweld) Splices in Reinforcing Bars of Category I Concrete Structure.

3.8.3.6.8 Construction Codes of Practice

The following codes of practice establish the standards of construction procedure:

a. ACI 301-72, "Specifications for Structural Concrete for Buildings"

b. ACI 305, "Recommended Practice for Hot-Weather Concreting"

c. ACI 306, "Recommended Practice for Cold-Weather Concreting"

d. ACI 308, "Recommended Practice for Curing Concrete"

e. ACI 318, "Building Code Requirements for Reinforced Concrete"

f. ACI 614, "Recommended Practice for Measuring Mixing, Transporting, and Placing Concrete"

g. ACI 315, "Manual of Standard Practice for Detailing Reinforced Concrete Structures"

h. AWS D1.1, "Code for Welding in Building Construction"

i. AISC Manual of Steel Construction including all specifications contained therein.

In every instance, the construction procedure equals or exceeds the recommendations set forth in the foregoing publications.

3.8.3.6.9 Reflective Insulation in the SSW/RPV Annulus

Reflective insulation is of all metallic construction consisting of sheets of ASTM A 167 or A 240 stainless steel type 304 or aluminum alloy No. 3003, or a combination of both with stainless steel on the exterior and interior surfaces. There are no organic materials or leachable chlorides in the completed insulation. Accessories including locking devices are AISI type 300 stainless steel; AISI type 400 stainless steel is used for threaded fasteners to prevent galling. Materials are non-combustible. Insulation is not greater than 3½ inches thick.

3.8.3.6.10 Reflective Insulation Inside the RPV Skirt

Material and construction of reflective insulation inside the RPV skirt is essentially the same as the reflective insulation described in 3.8.3.6.9. This insulation is approximately 3 inches thick.

3.8.3.7 Testing and Inservice Surveillance Requirements

There are no testing or inservice surveillance requirements for the structures discussed in this report, i.e., the SSW to RPV pedestal connection, the RPV skirt to pedestal connection, and the upper portion of the RPV pedestal.

REFERENCES

1. R.B. McClintock and G.J. Silvestri, "Some Improved Steam Property Calculation Procedures", ASME Transactions, Journal of Engineering for Power, pages 92, 123, (1970).

2. 1967 ASME Steam Tables.

3. Crane Co. "Flow of Fluids Through Valves, Fittings and Pipe", Crane Co. Technical Paper, No. 410, 1967.

4. Lewis F. Moody, "Friction Factors for Pipe Flow", Transactions ASME Volume 66, No. 8, November 1944.

5. F.J. Patti (Burns and Roe) letter to J. Kudrick (AEC) of September 27, 1974, "13 Benchmark Problems for Sub-compartment Analysis".

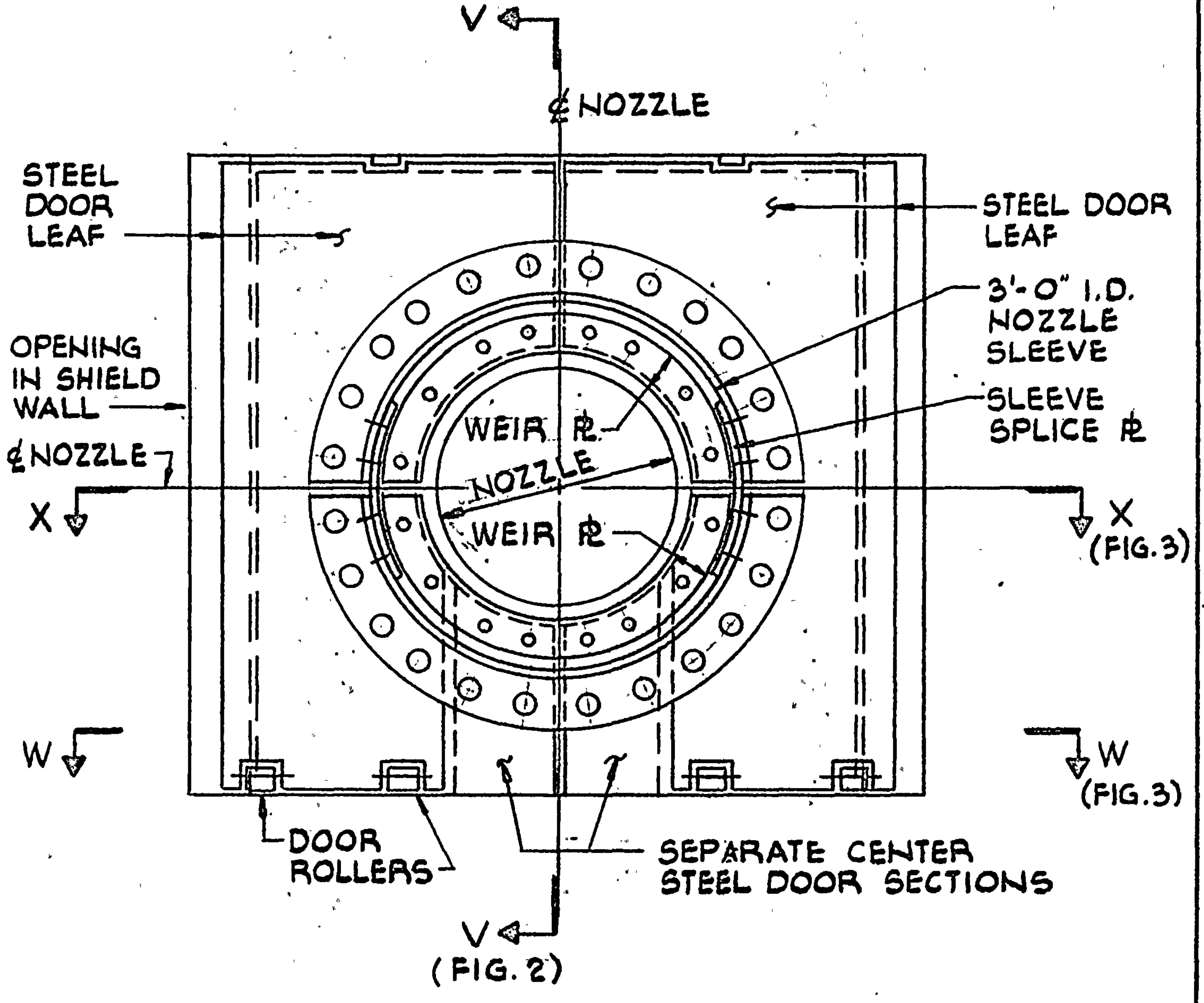

VIEW OF OUTBOARD FACE OF STEEL DOOR

NOTE: PERMALI NOT SHOWN

WASHINGTON PUBLIC POWER SUPPLY SYSTEM NUCLEAR PROJECT NO. 2	24" RECIRCULATION LINE SHIELD WALL DOOR DESIGN	FIGURE 1

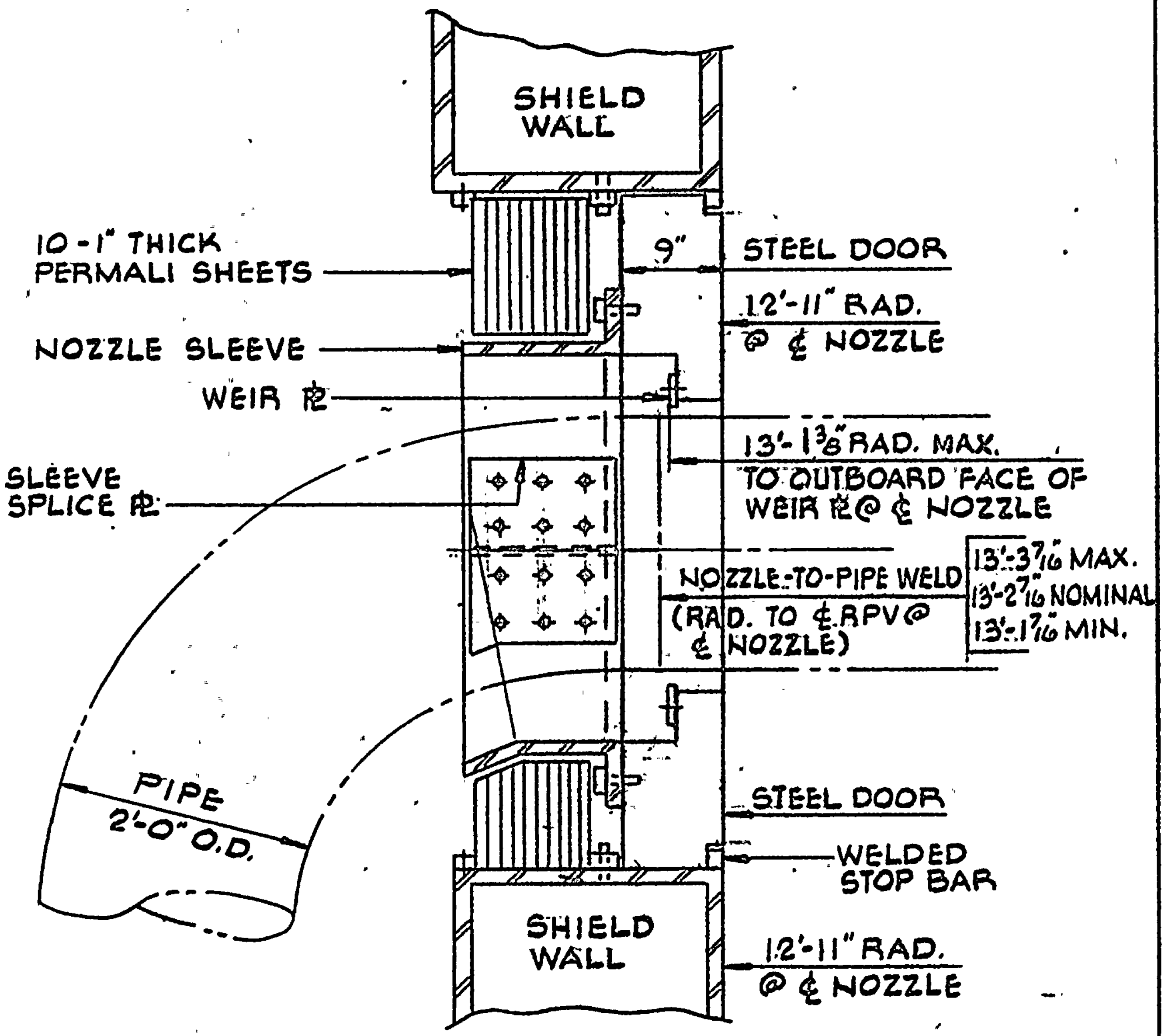

SECTIONAL ELEVATION V-V
CUT FROM FIG. 1

WASHINGTON PUBLIC POWER SUPPLY SYSTEM NUCLEAR PROJECT NO. 2	24" RECIRCULATION LINE SHIELD WALL DOOR DESIGN	FIGURE 2

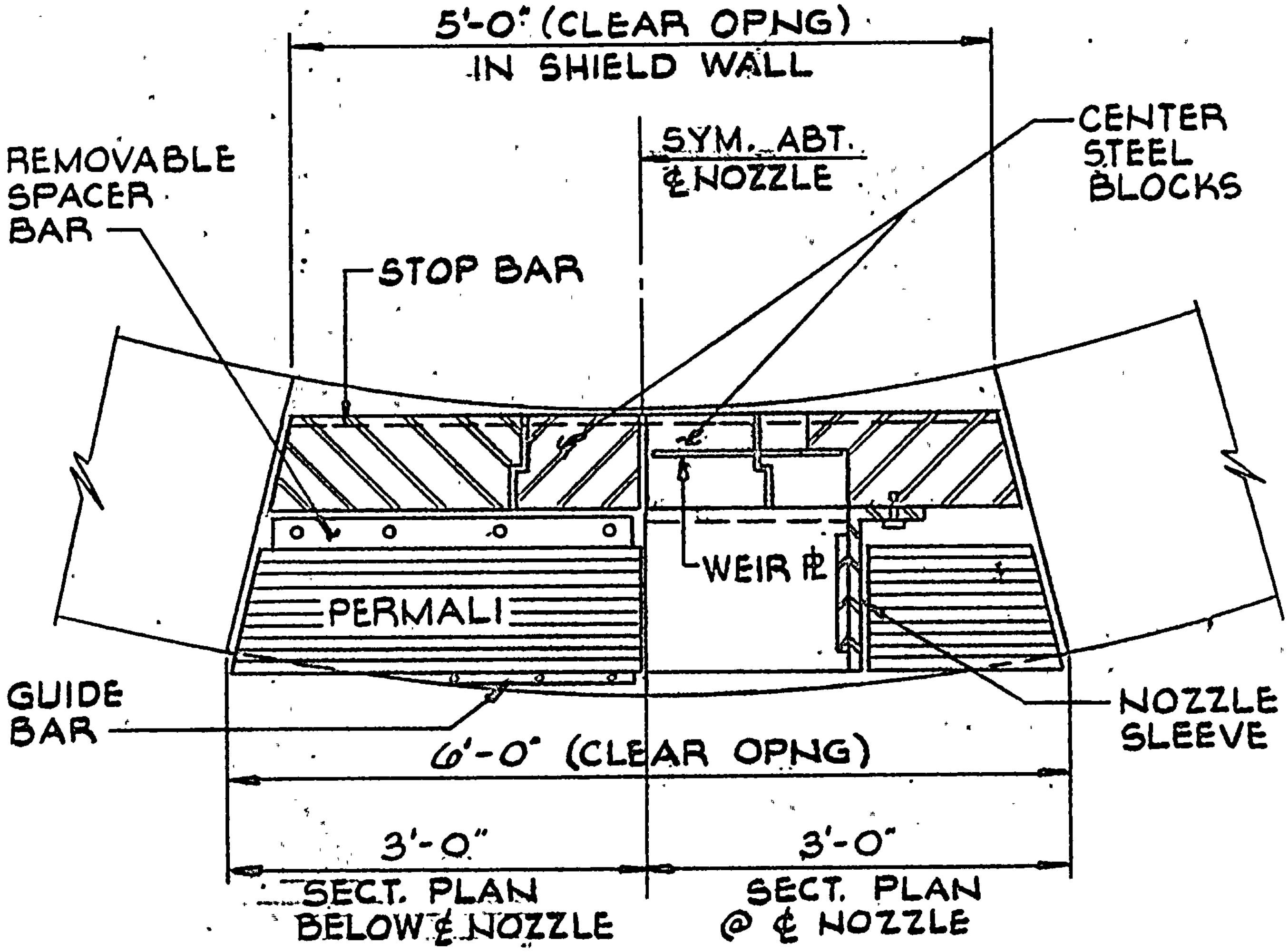

SECT. W-W
FROM FIG. 1

SECT. X-X
FROM FIG. 1

NOTE: NOZZLE NOT SHOWN

WASHINGTON PUBLIC POWER SUPPLY SYSTEM NUCLEAR PROJECT NO. 2	24" RECIRCULATION LINE SHIELD WALL DOOR DESIGN	FIGURE 3

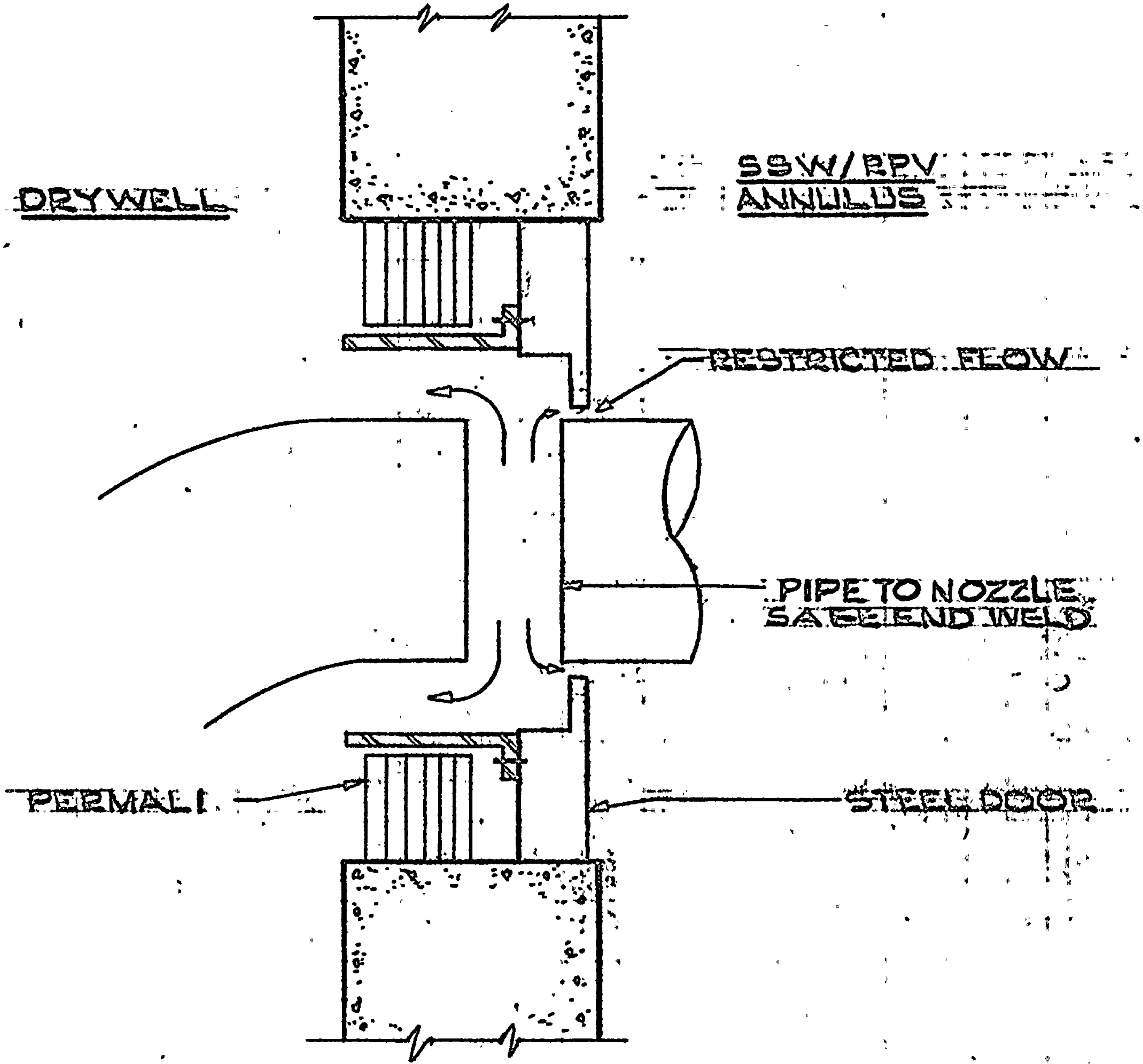

WASHINGTON PUBLIC POWER SUPPLY SYSTEM NUCLEAR PROJECT NO. 2	FLOW SPLIT FOLLOWING PIPE BREAK	FIGURE 4

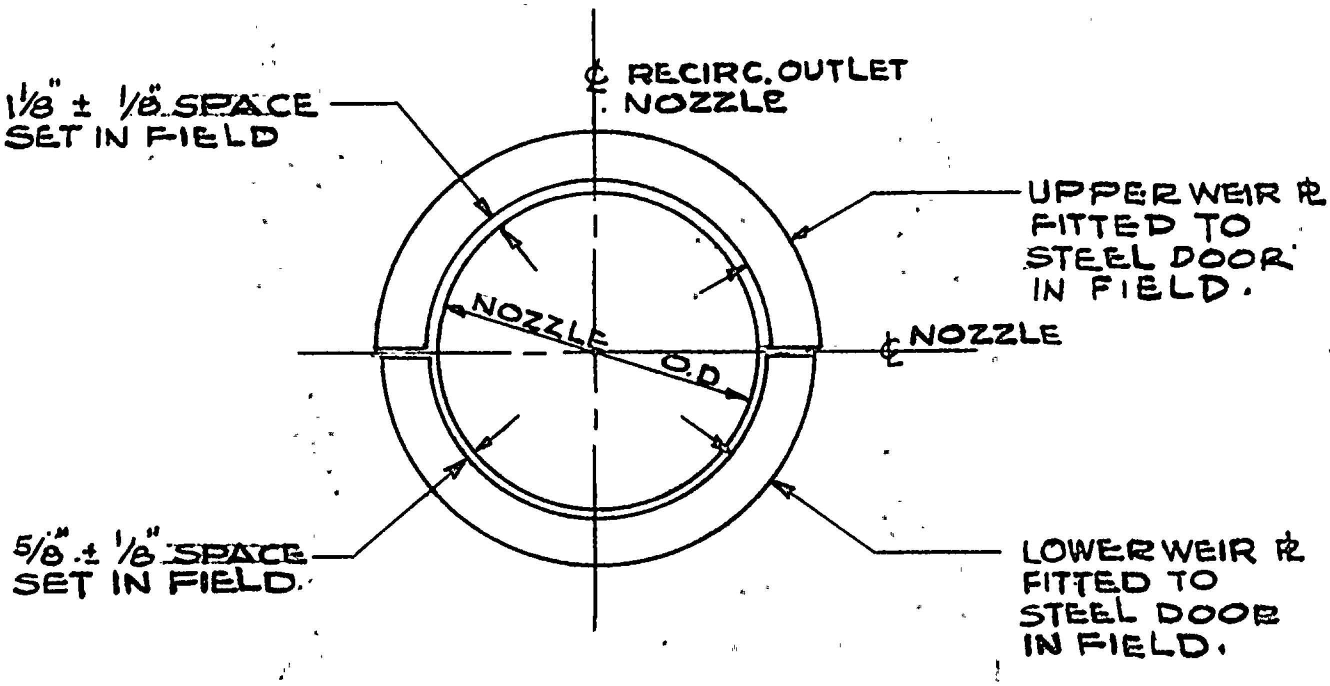

VIEW OF OUTBOARD FACE OF WEIR PLATES.

WASHINGTON PUBLIC POWER SUPPLY SYSTEM NUCLEAR PROJECT NO. 2	WEIR PLATE FIT-UP	FIGURE 5

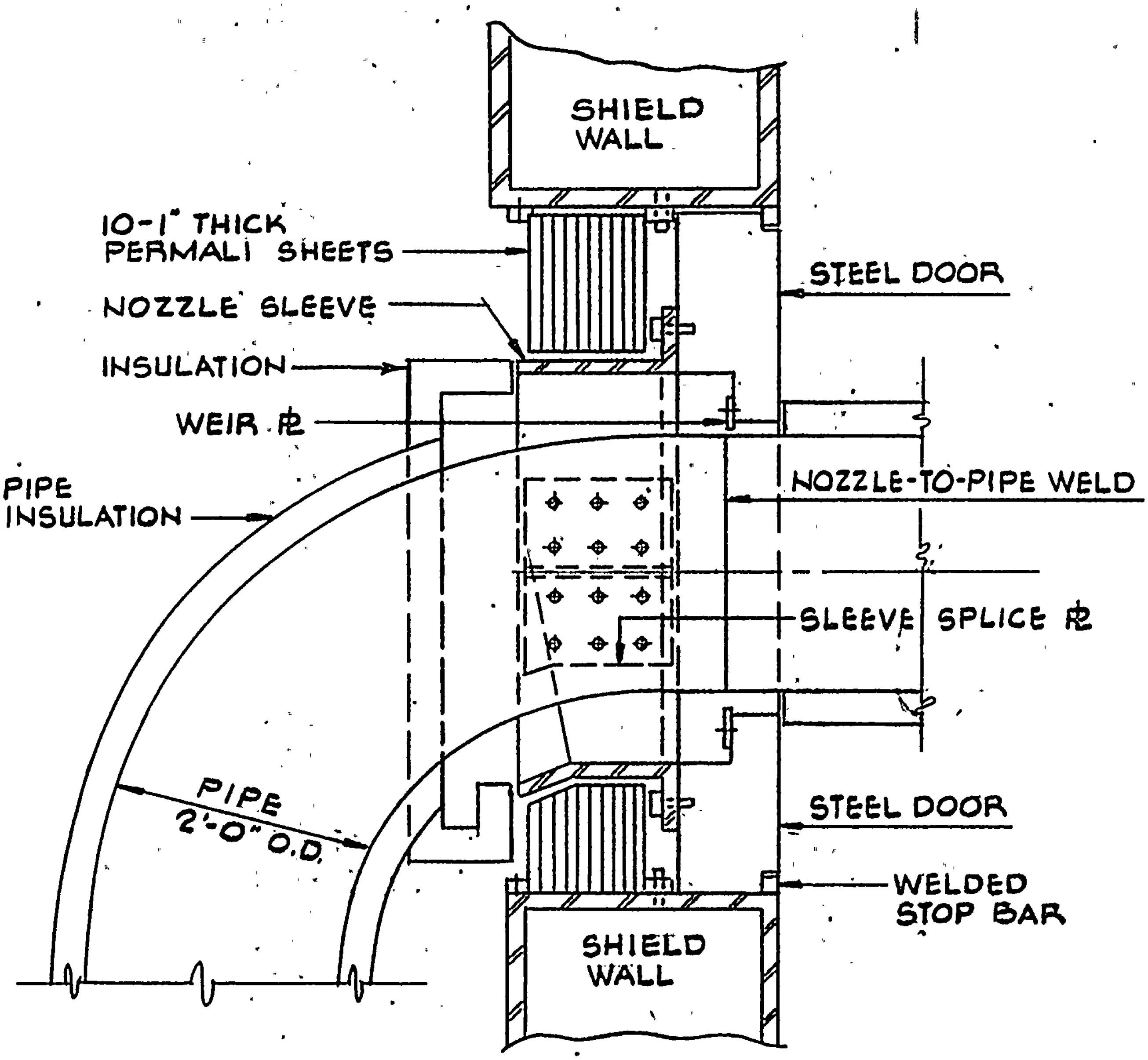

SECTIONAL ELEVATION V-V
CUT FROM FIG. I

WASHINGTON PUBLIC POWER SUPPLY SYSTEM NUCLEAR PROJECT NO. 2	24" RECIRCULATION LINE SHIELD WALL DOOR DESIGN, PIPE INSULATION	FIGURE 6

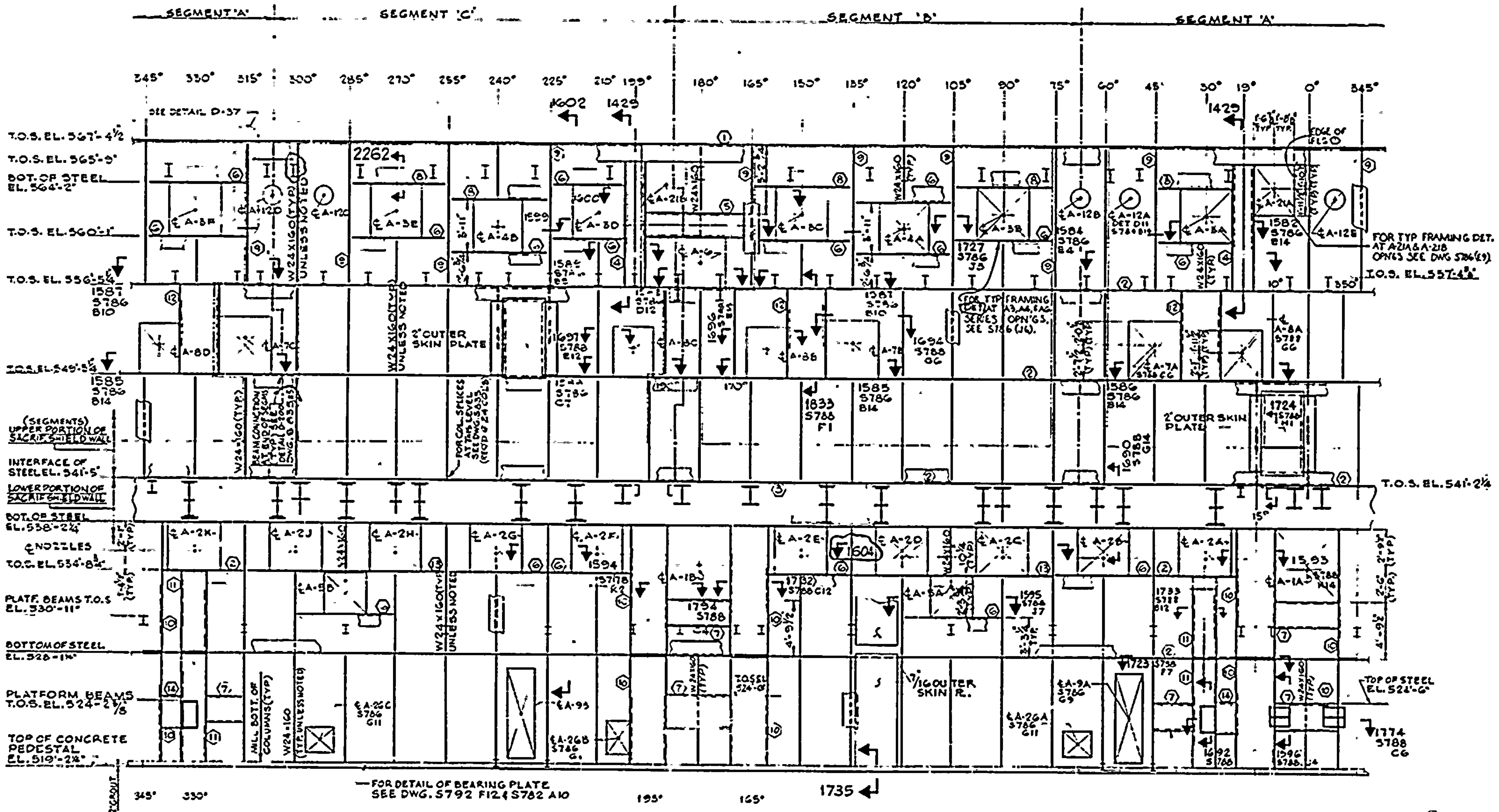

LEGEND:
— — — DENOTES DIVISION BETWEEN SEGMENTS ON DWG. ABOVE
— · — · — DENOTES THE LIMIT OF CONCRETE PLACEMENT AT UPPER PORTION OF SACRIFICIAL SHIELD WALL DURING LIFTING OPERATIONS.

FLAT DEVELOPMENT OF SHIELDWALL AT OUTBOARD FACE
SCALE: 1/4" = 1'-0"

TABULATION OF SHIELDWALL OPENINGS

IDENTIFICATION Nº	Nº OF OPNGS	EL. OF ℄ NOZZLE OR PIPE	AZIMUTH OF NOZZLE	CLEAR OPNG. SIZE* HEIGHT	WIDTH
A-1A & A-1B	2	535'-4¾	0° & 180°	5'-3½	5'-0"
A-2A, A-2B, A-2C, A-2D, A-2E, A-2F, A-2G, A-2H, A-2J, A-2K	10	536'-1¼	AS NOTED ON DEVELOPED ELEVATION	3'-5½	4'-1"
A-3A, A-3B, A-3C, A-3D, A-3E, A-3F	6	562'-1½	30°, 90°, 150°, 210°, 270°, 330°	4'-1"	4'-1"
A-4A & A-4B	2	560'-11½	120°, 240°	3'-11"	3'-11"
A-5A & A-5B	2	533'-8¼	105°, 285°	3'-2"	3'-4½
A-6	1	558'-4¾	180°	3'-11"	3'-11"
A-7A, A-7B, A-7C	3	552'-0¾	45°, 135°, 315°	4'-8"	4'-1"
A-8A, A-8B, A-8C, A-8D	4	551'-6¼	20°, 160°, 200°, 340°	4'-0½	3'-2½
A-9A & A-9B	2	523'-6¼	52°-30', 232°-30'	7'-0"	2'-4"
A-12A, A-12B, A-12C, A-12D, A-12E	5	563'-5"	52°30', 67°30', 292°30', 307°-30', 352°-30'	1'-6" DIA.	
A-21A & A-21B	2	564'-1¼	10°, 190°	3'-9½	3'-3"
A-26A & A-26C	2	521'-4"	67°-30', 292°-30'	2'-0"	2'-2"
A-26B	1	521'-8"	203°-36'	2'-6"	1'-8"

* ℄ OF OPENING

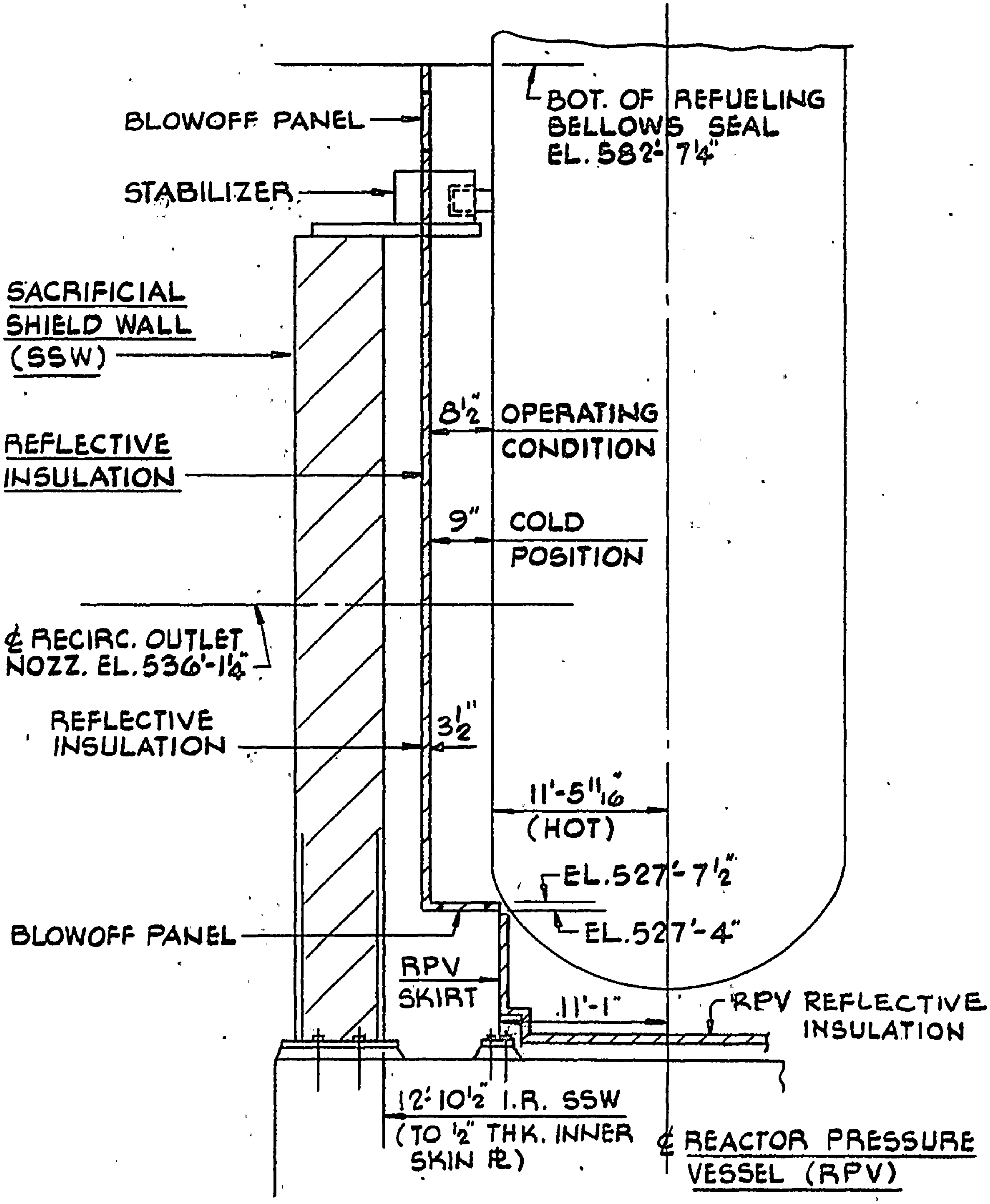

WASHINGTON PUBLIC POWER SUPPLY SYSTEM NUCLEAR PROJECT NO. 2	RPV/SSW ANNULAR SPACE	FIGURE 8

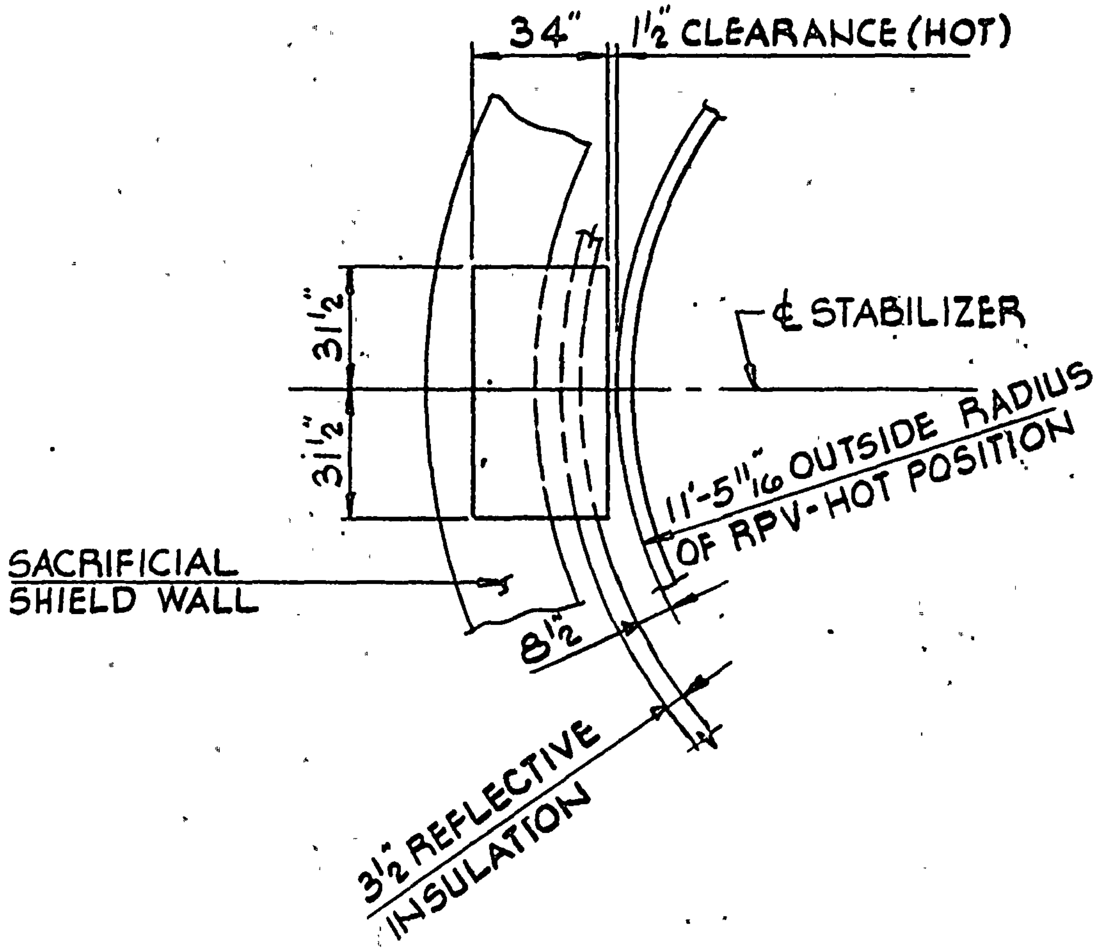

WASHINGTON PUBLIC POWER SUPPLY SYSTEM NUCLEAR PROJECT NO. 2	RPV STABILIZER - PLAN VIEW	FIGURE 9

IDENTIFICATION No.	PIPE SIZE	FUNCTION
A-1A, A-1B	24"	RECIRCULATION OUTLETS
A-2A, A-2B, A-2C, A-2D, A-2E, A-2F A-2G, A-2H, A-2J A-2K	12"	RECIRCULATION INLETS
A-3A, A-3B, A-3C, A-3D, A-3E, A-3F	12"	FEEDWATER
A-4A, A-4B	10"	LPCS, HPCS
A-5A, A-5B	4"	JET PUMP INSTR.
A-6	3"	CRD HYD. SYSTEM
A-7A, A-7B, A-7C	12"	RHR/LPCI
A-8A, A-8B, A-8C, A-8D	2"	INSTRUMENTATION, WATER LEVEL
A-9A, A-9B	NO PIPING	INSPECTION DOORS
A-12A, A-12B, A-12C, A-12D, A-12E	NO PIPING	VENTILATION OPENINGS
A-21A, A-21B	2"	INSTRUMENTATION, WATER LEVEL
A-26A, A-26B, A-26C, A-26D	NO PIPING	VENTILATION DUCTS

PIPE INSULATION – 3" THICKNESS

WASHINGTON PUBLIC POWER SUPPLY SYSTEM NUCLEAR PROJECT NO. 2	SHIELD WALL OPENINGS	FIGURE 10

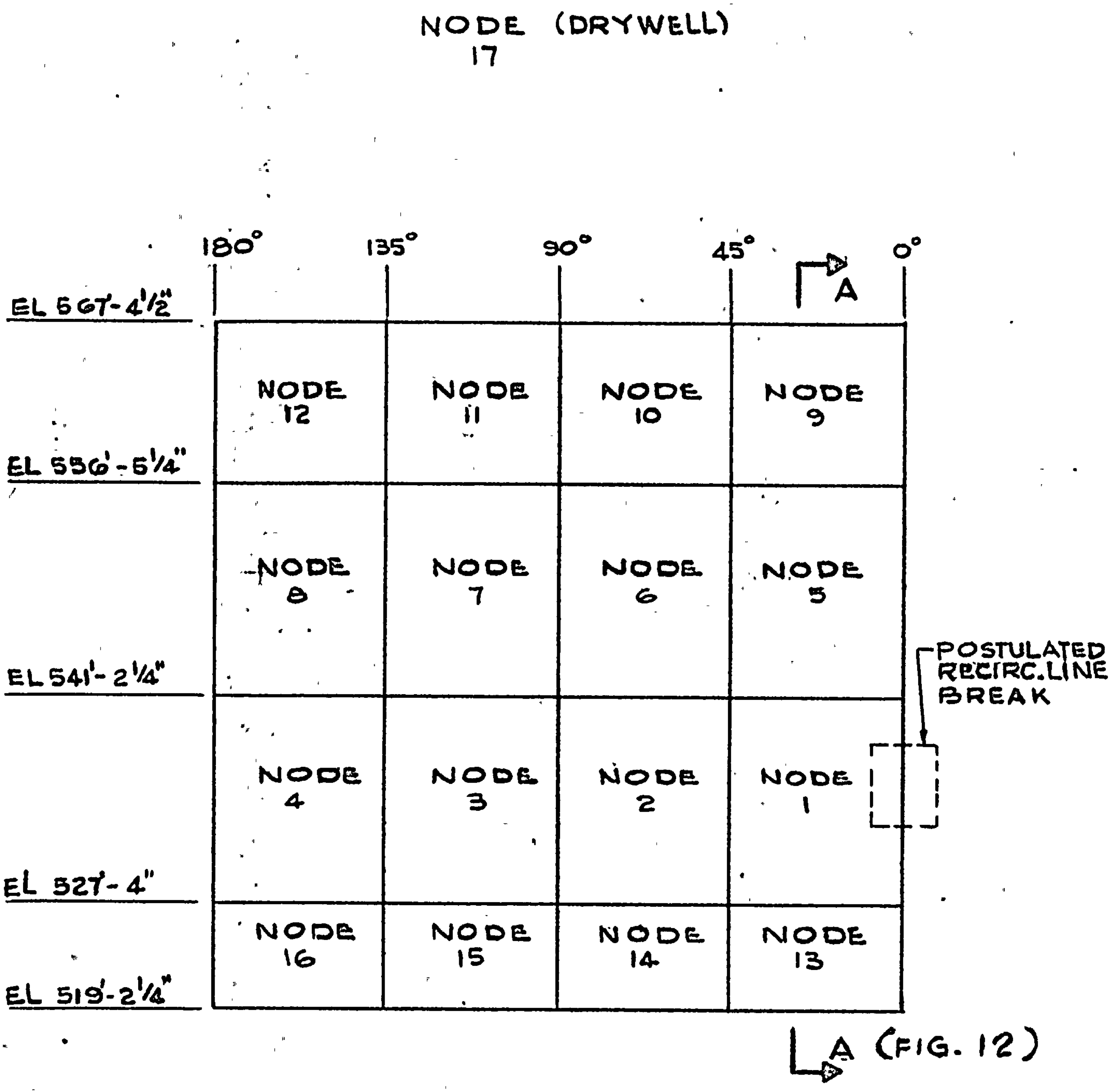

180° FLAT DEVELOPMENT OF SHIELD WALL ANNULUS

WASHINGTON PUBLIC POWER SUPPLY SYSTEM NUCLEAR PROJECT NO. 2	SHIELD WALL ANNULUS NODAL ARRANGEMENT	FIGURE 11

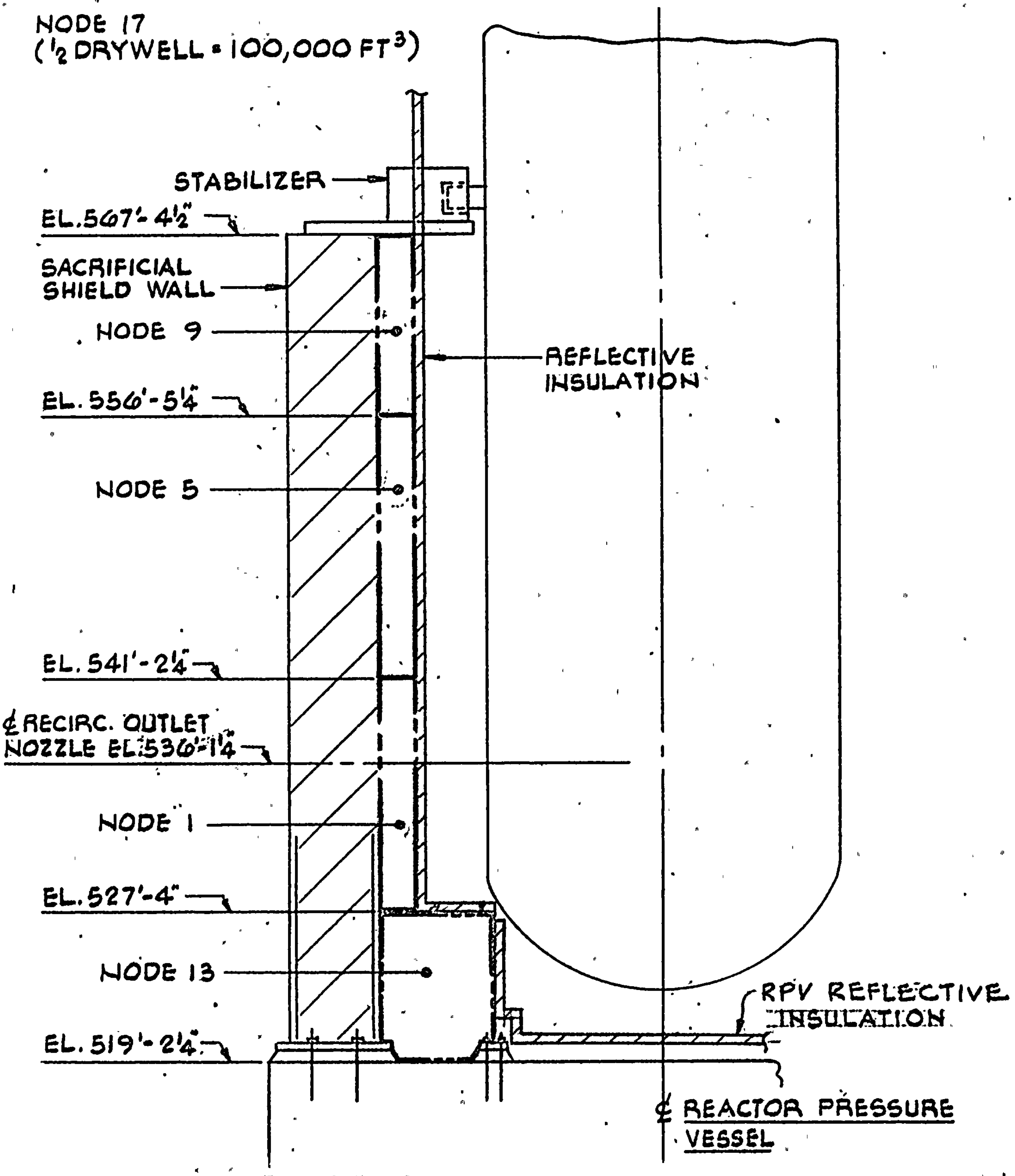

SECTION A-A

CUT FROM FIG. 11

WASHINGTON PUBLIC POWER SUPPLY SYSTEM NUCLEAR PROJECT NO. 2	SHIELD WALL ANNULUS NODAL ARRANGEMENT	FIGURE 12

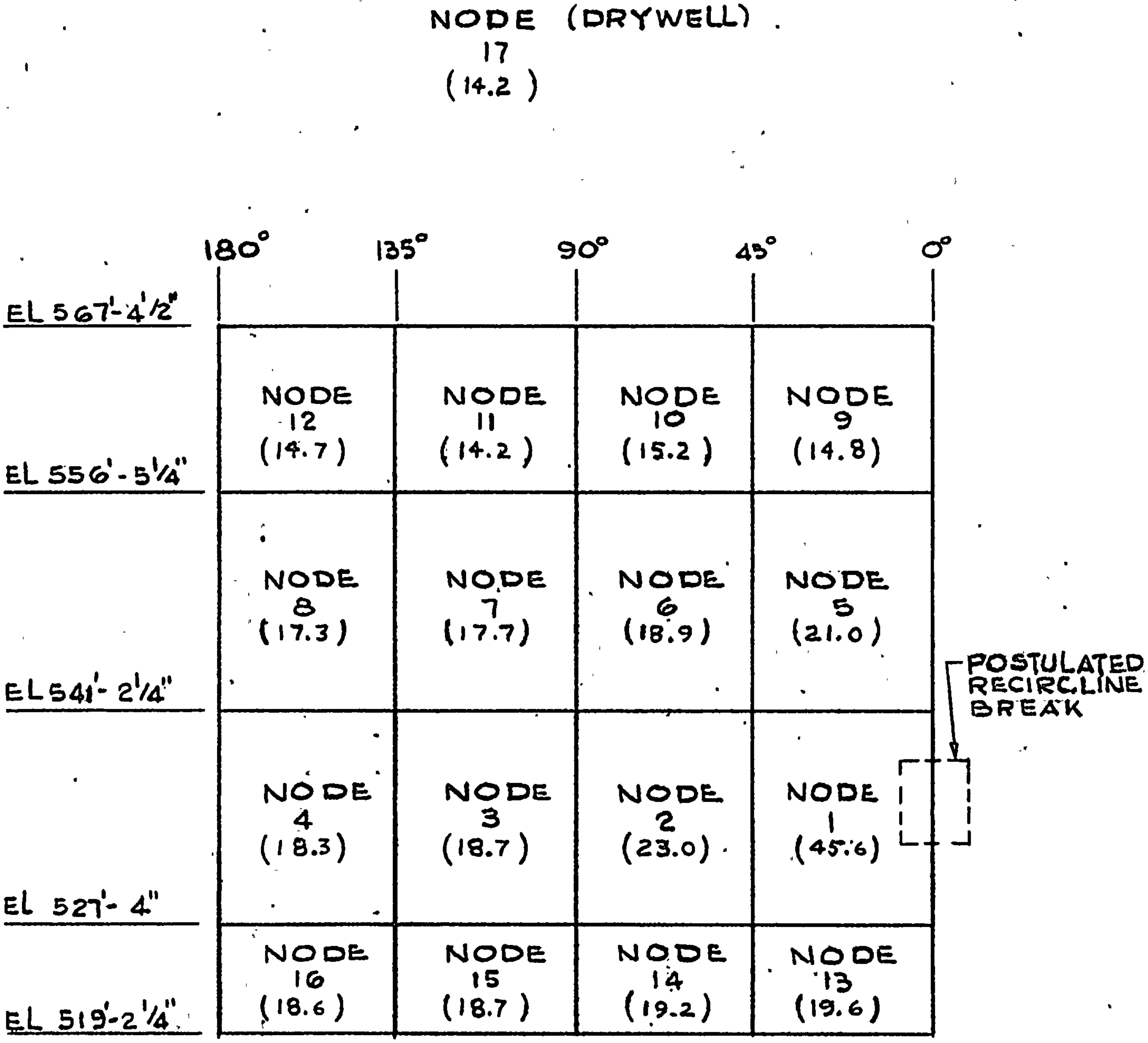

180° FLAT DEVELOPMENT OF SHIELD WALL ANNULUS

( ) = PRESSURE [PSIA]

WASHINGTON PUBLIC POWER SUPPLY SYSTEM NUCLEAR PROJECT NO. 2	PRESSURE DISTRIBUTION 34 NODE CASE	FIGURE 13

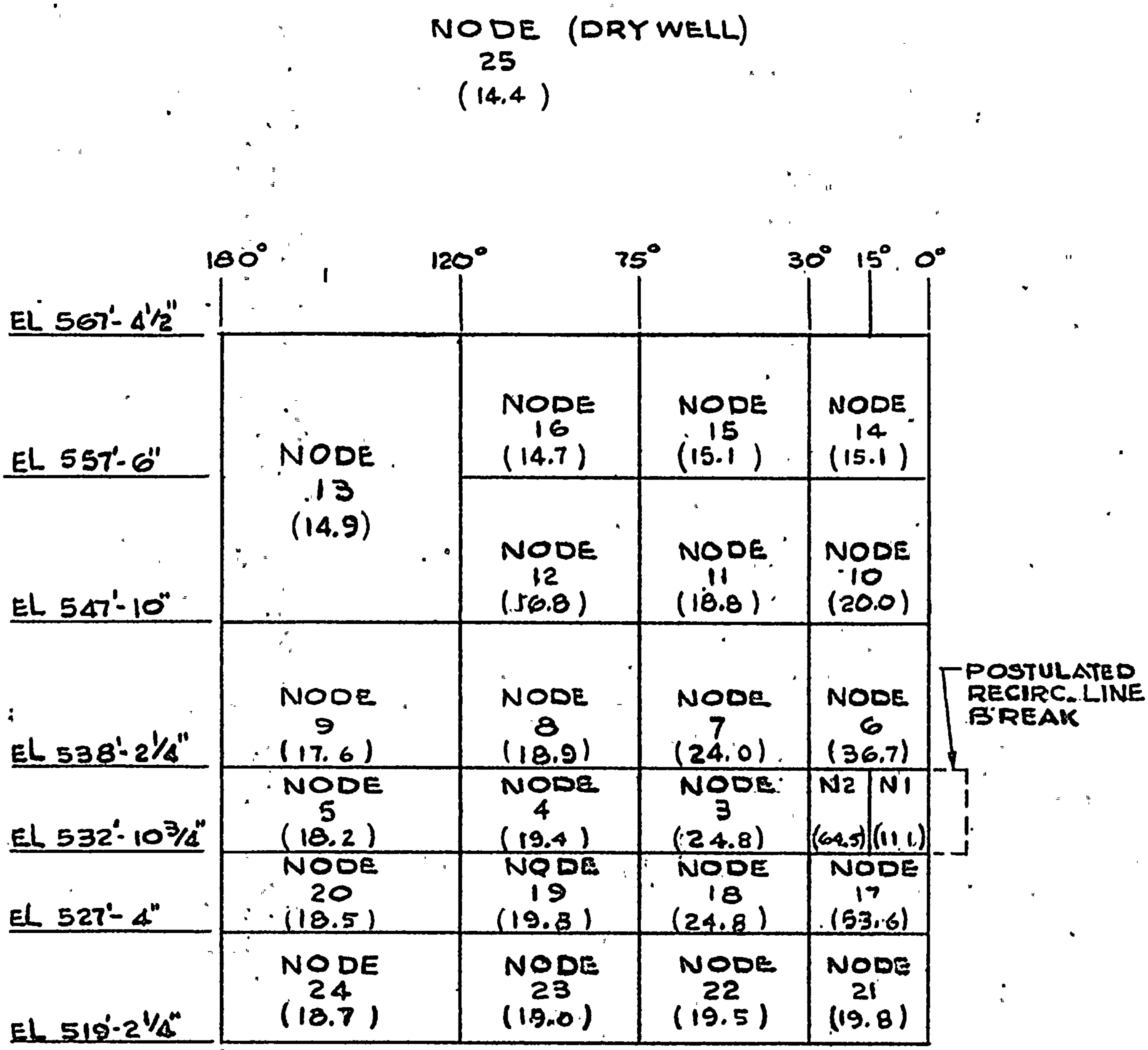

180° FLAT DEVELOPMENT OF SHIELD WALL ANNULUS

(   ) = PRESSURE [PSIA]

WASHINGTON PUBLIC POWER SUPPLY SYSTEM NUCLEAR PROJECT NO. 2	PRESSURE DISTRIBUTION 50 NODE CASE	FIGURE 14

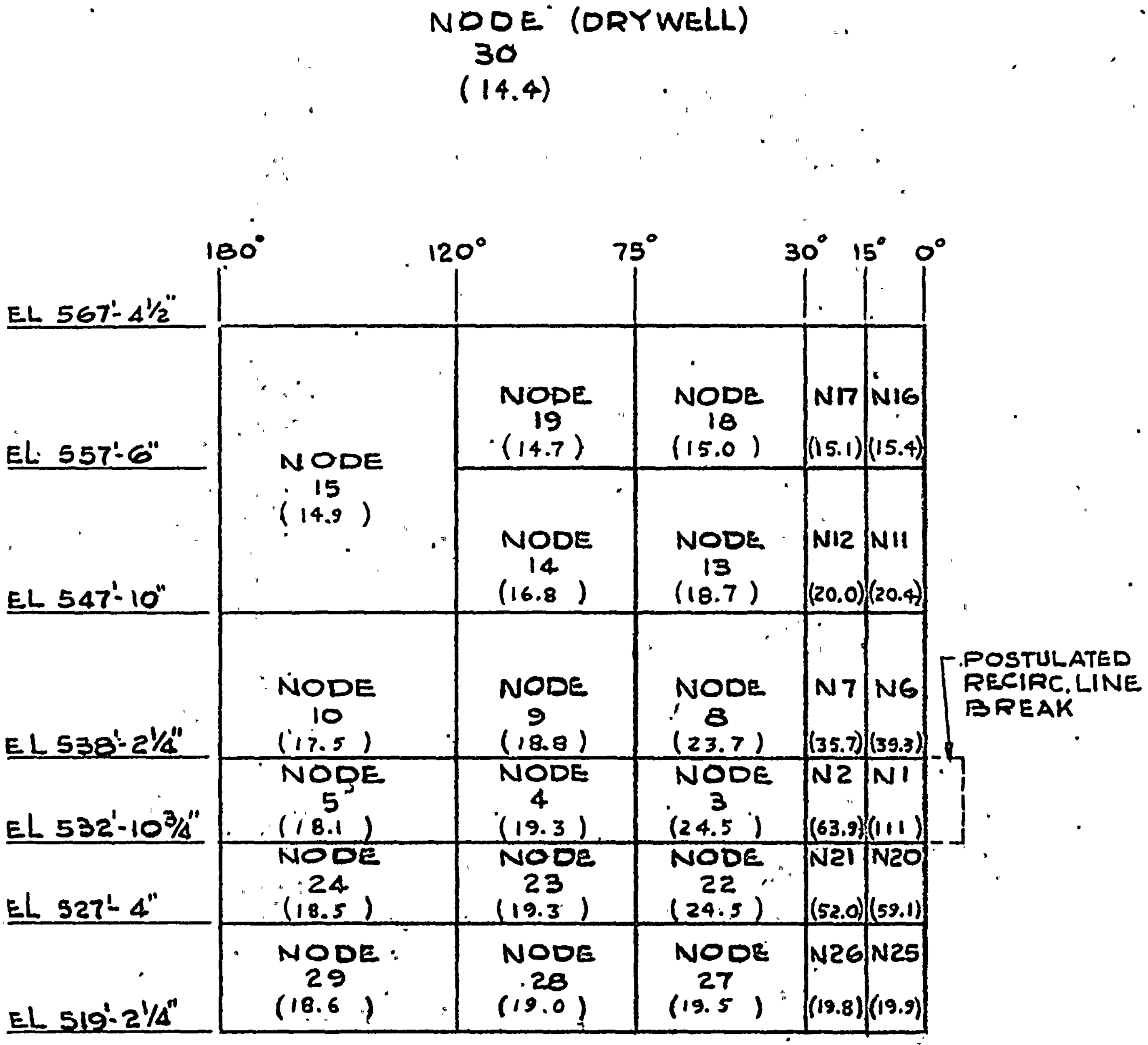

180° FLAT DEVELOPMENT OF SHIELD WALL ANNULUS

( ) = PRESSURE [P.S.I.A]

WASHINGTON PUBLIC POWER SUPPLY SYSTEM NUCLEAR PROJECT NO. 2	PRESSURE DISTRIBUTION 60 NODE CASE	FIGURE 15

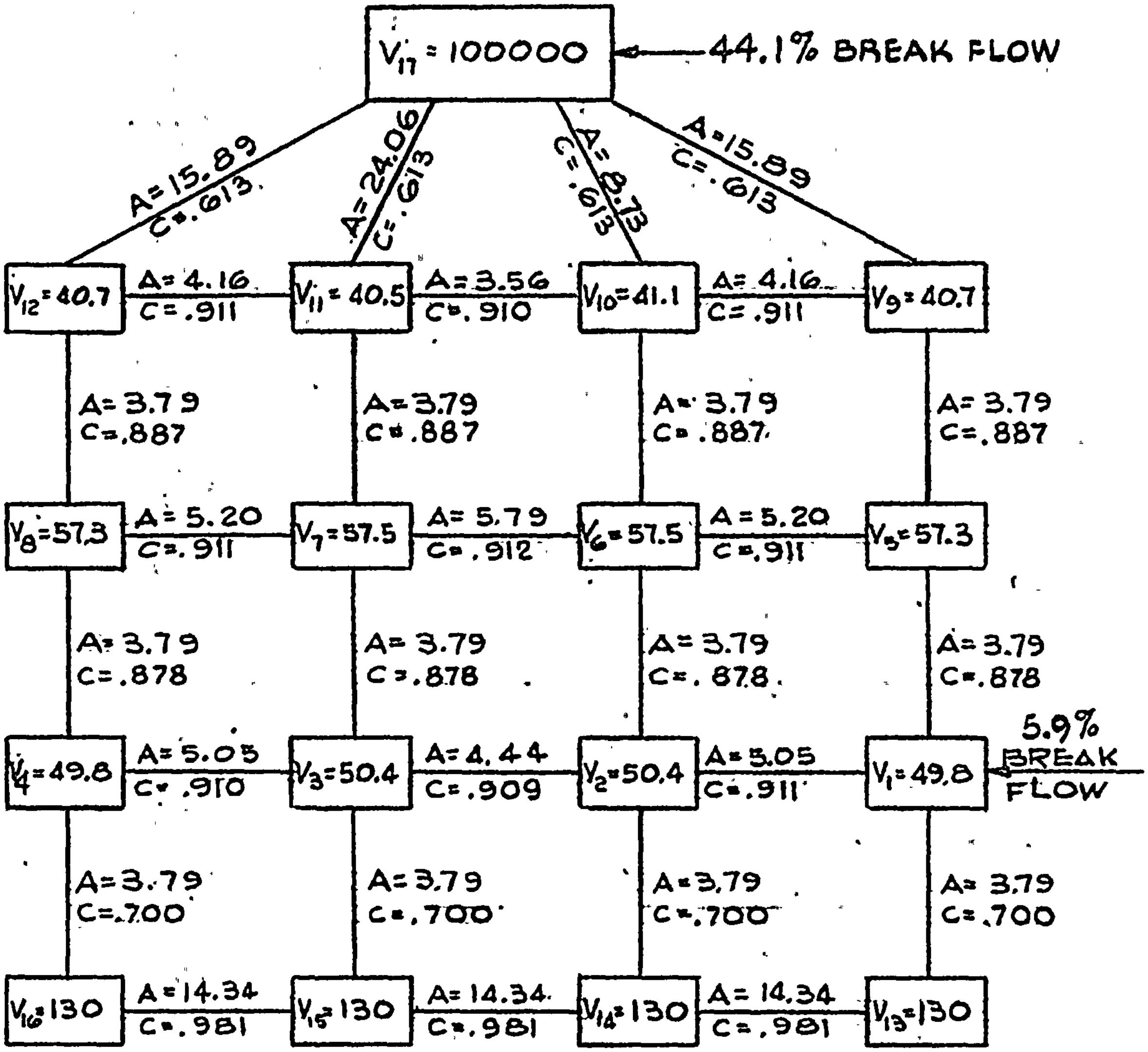

V= COMPARTMENT VOLUME [ft^3]

A= VENT AREA [ft^2]

C= FLOW COEFFICIENT [DIMENSIONLESS]

WASHINGTON PUBLIC POWER SUPPLY SYSTEM NUCLEAR PROJECT NO. 2	SCHEMATIC FLOW DIAGRAM 34 NODE CASE	FIGURE 16

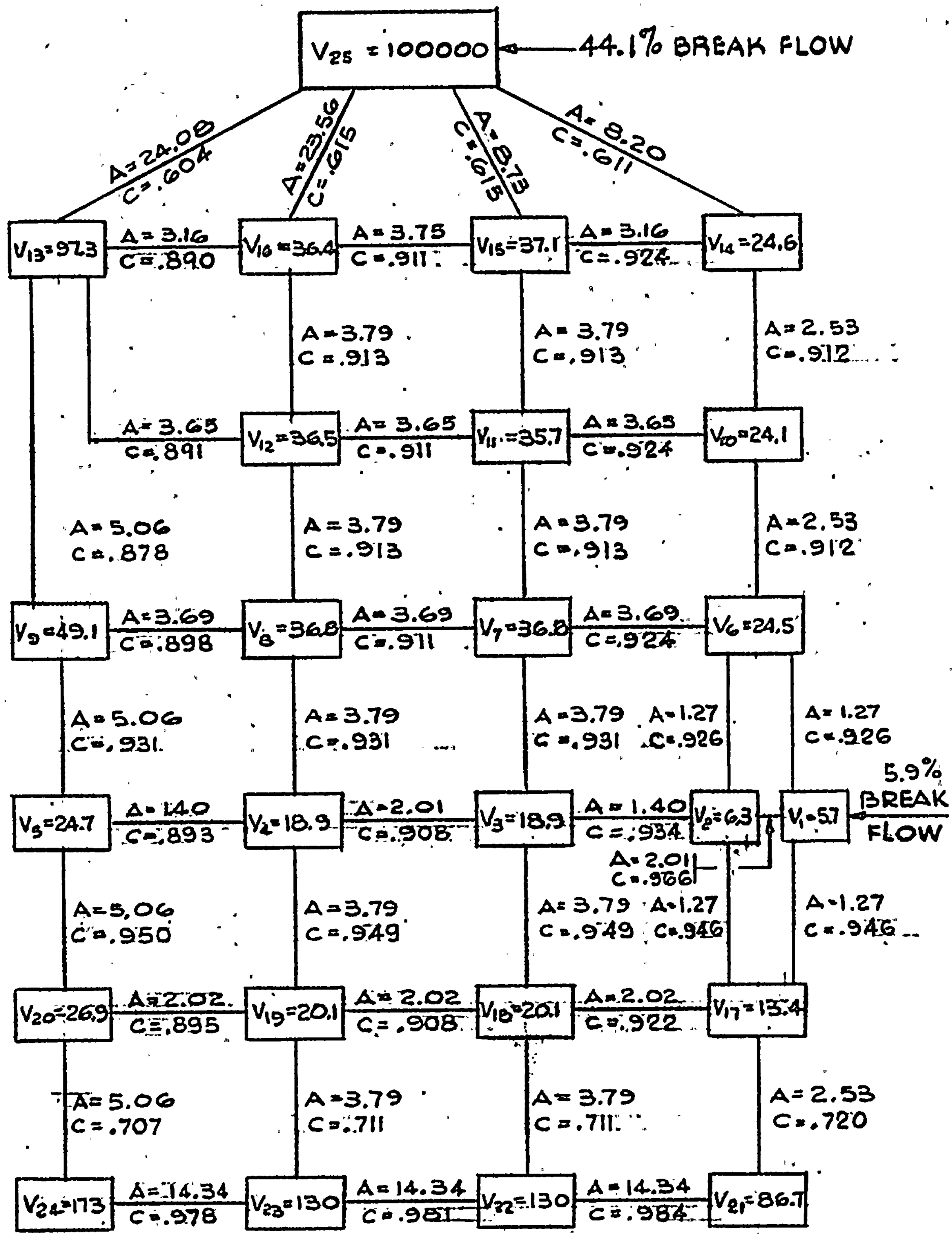

V = COMPARTMENT VOLUME [ft^3]

A = VENT AREA [ft^2]

C = FLOW COEFFICIENT [DIMENSIONLESS]

WASHINGTON PUBLIC POWER SUPPLY SYSTEM NUCLEAR PROJECT NO. 2	SCHEMATIC FLOW DIAGRAM 50 NODE CASE	FIGURE 17

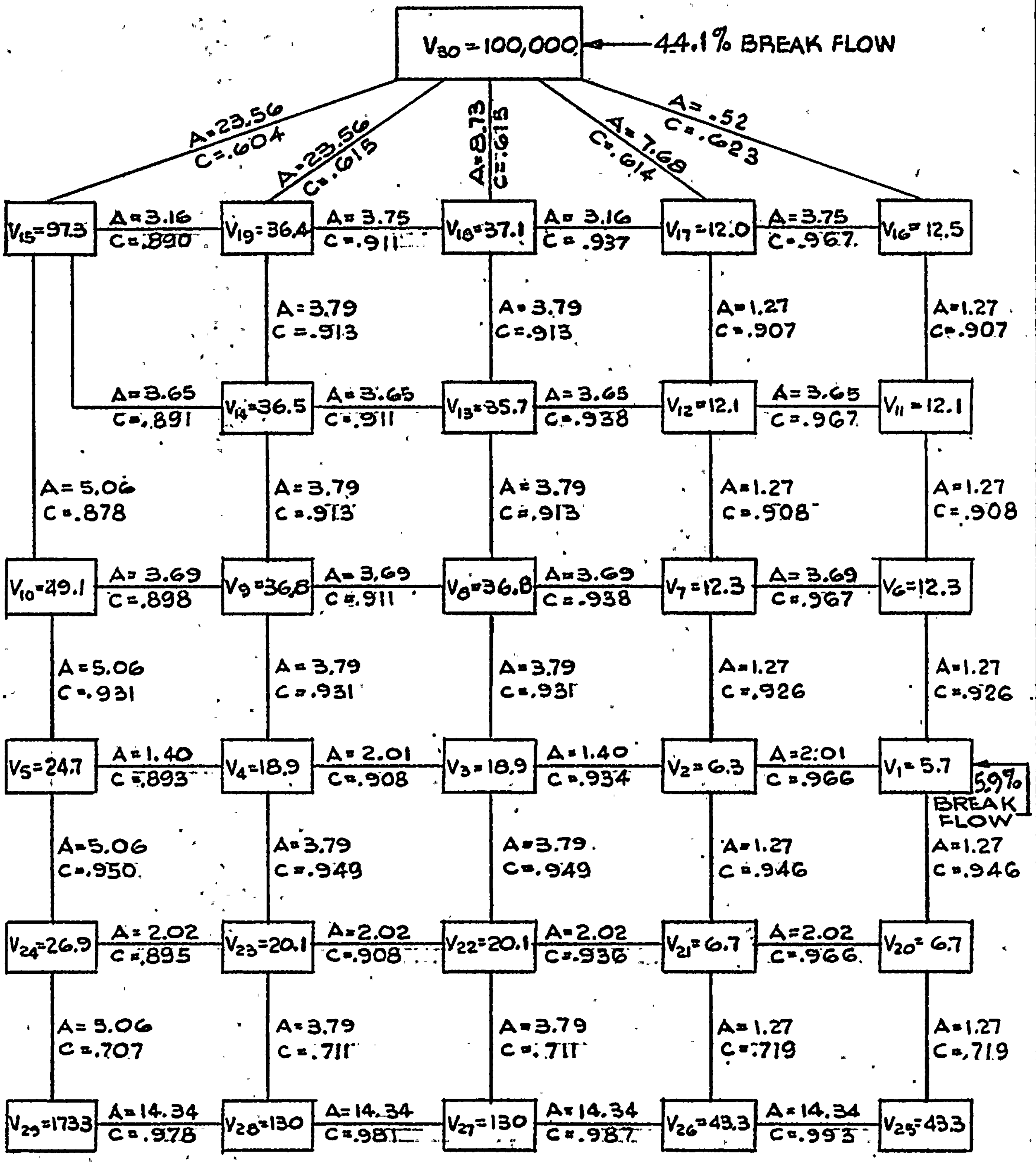

V = COMPARTMENT VOLUME [ft³]

A = VENT AREA [ft²]

C = FLOW COEFFICIENT [DIMENSIONLESS]

WASHINGTON PUBLIC POWER SUPPLY SYSTEM NUCLEAR PROJECT NO. 2	SCHEMATIC FLOW DIAGRAM 60 NODE CASE	FIGURE 18

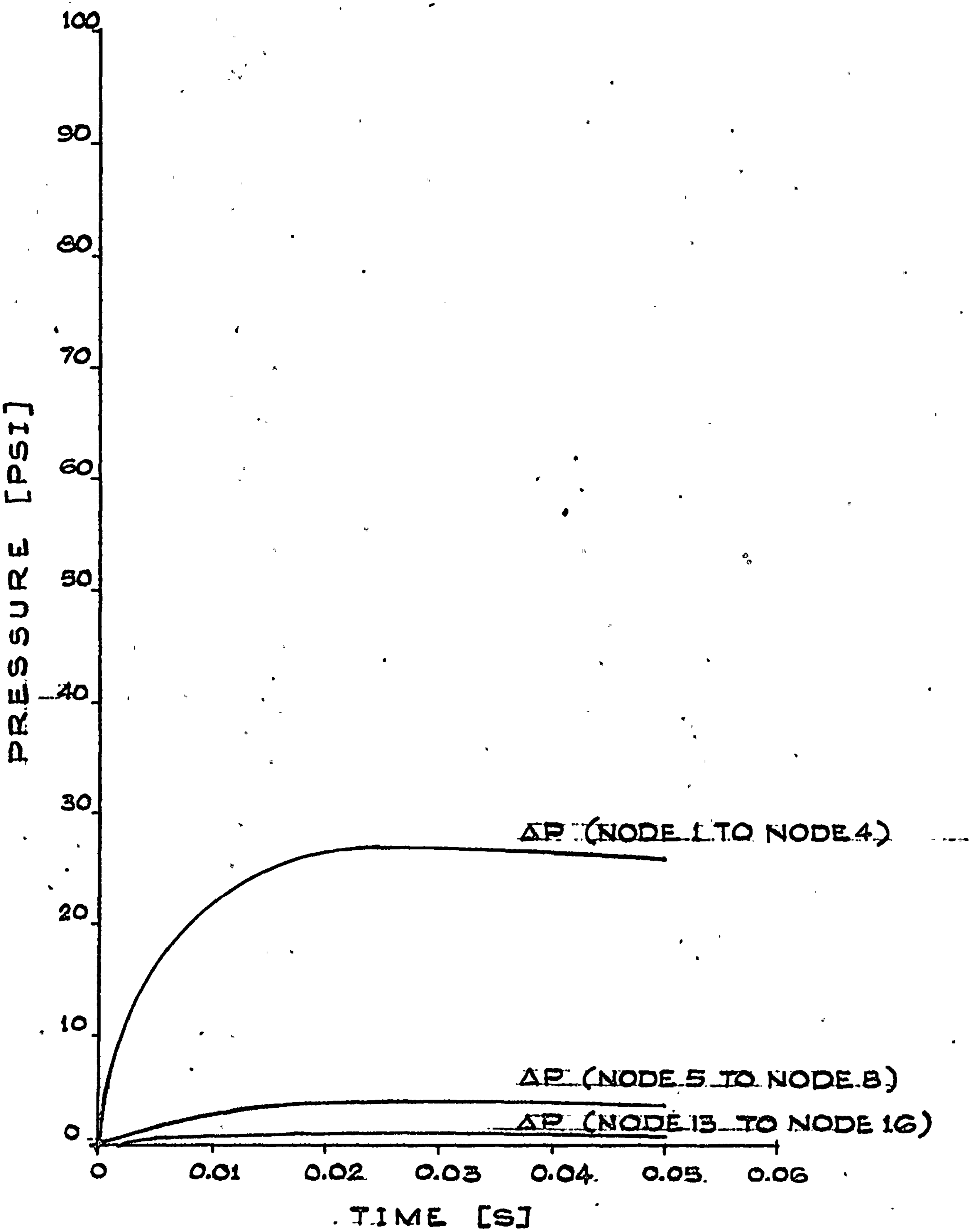

WASHINGTON PUBLIC POWER SUPPLY SYSTEM NUCLEAR PROJECT NO. 2	SHIELD WALL ANNULUS ΔP 17 NODE CASE	FIGURE 19

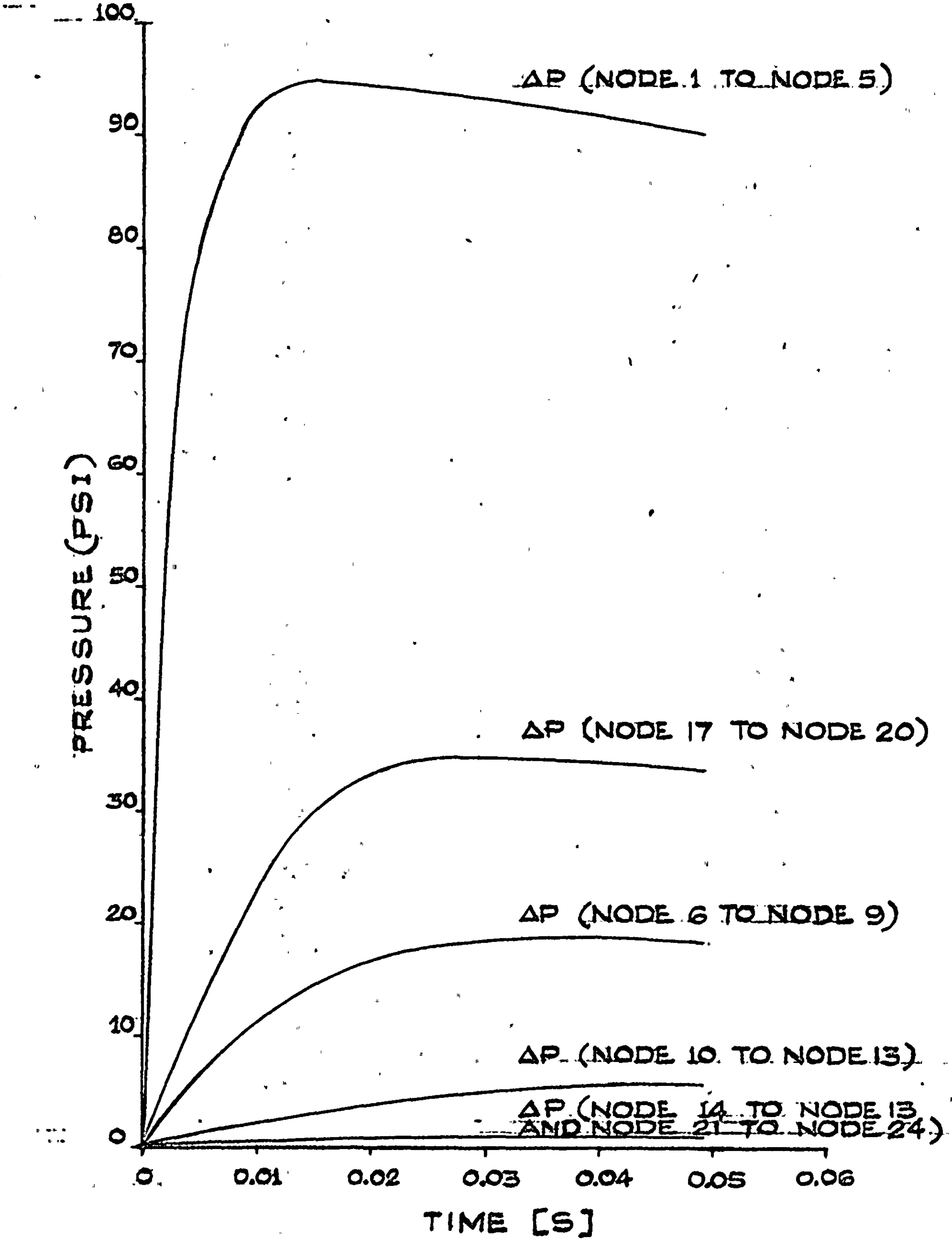

WASHINGTON PUBLIC POWER SUPPLY SYSTEM NUCLEAR PROJECT NO. 2	SHIELD WALL ANNULUS ΔP 50 NODE CASE	FIGURE 20

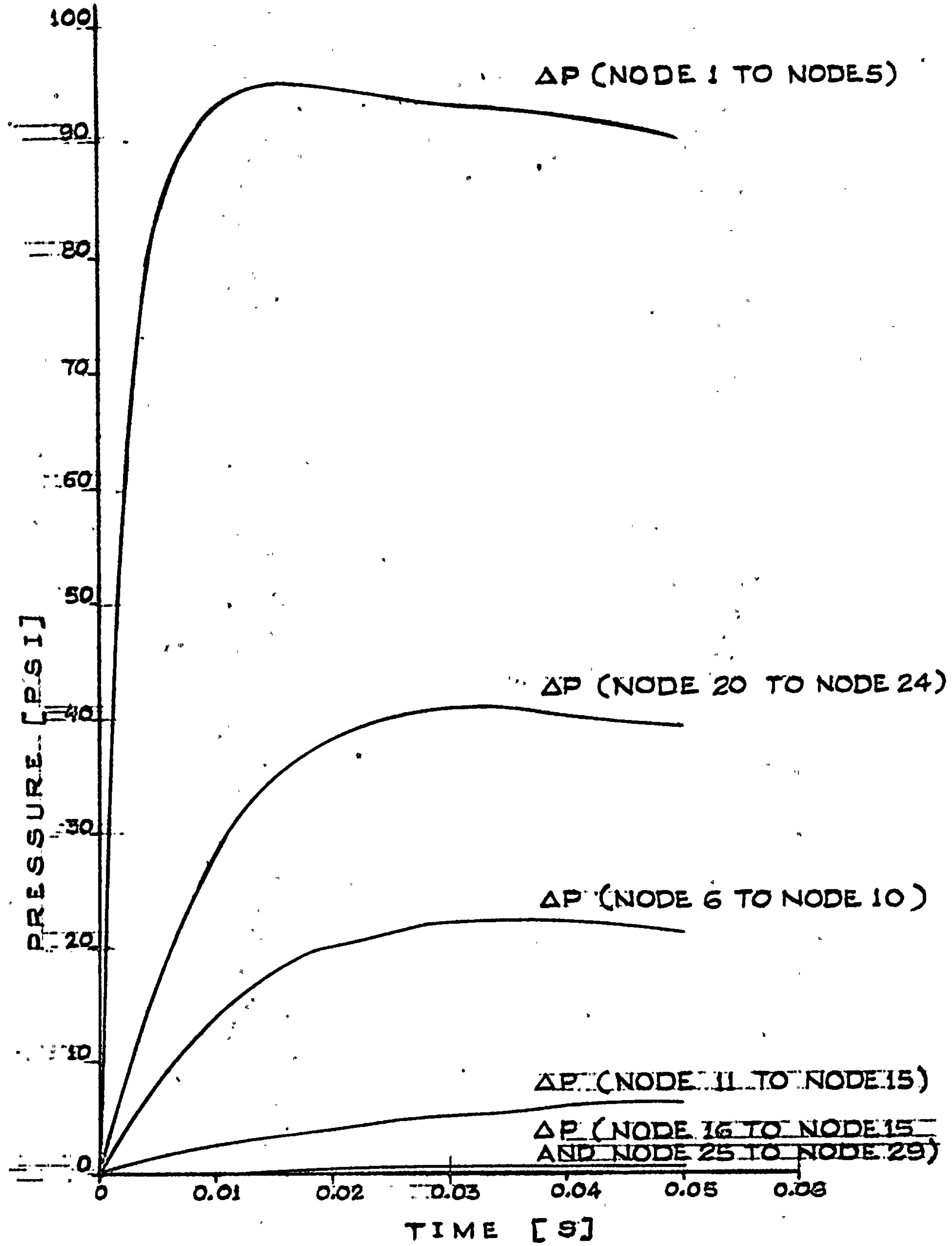

WASHINGTON PUBLIC POWER SUPPLY SYSTEM NUCLEAR PROJECT NO. 2	SHIELD WALL ANNULUS ΔP 60 NODE CASE, 7.5:1 FLOW SPLIT	FIGURE 21

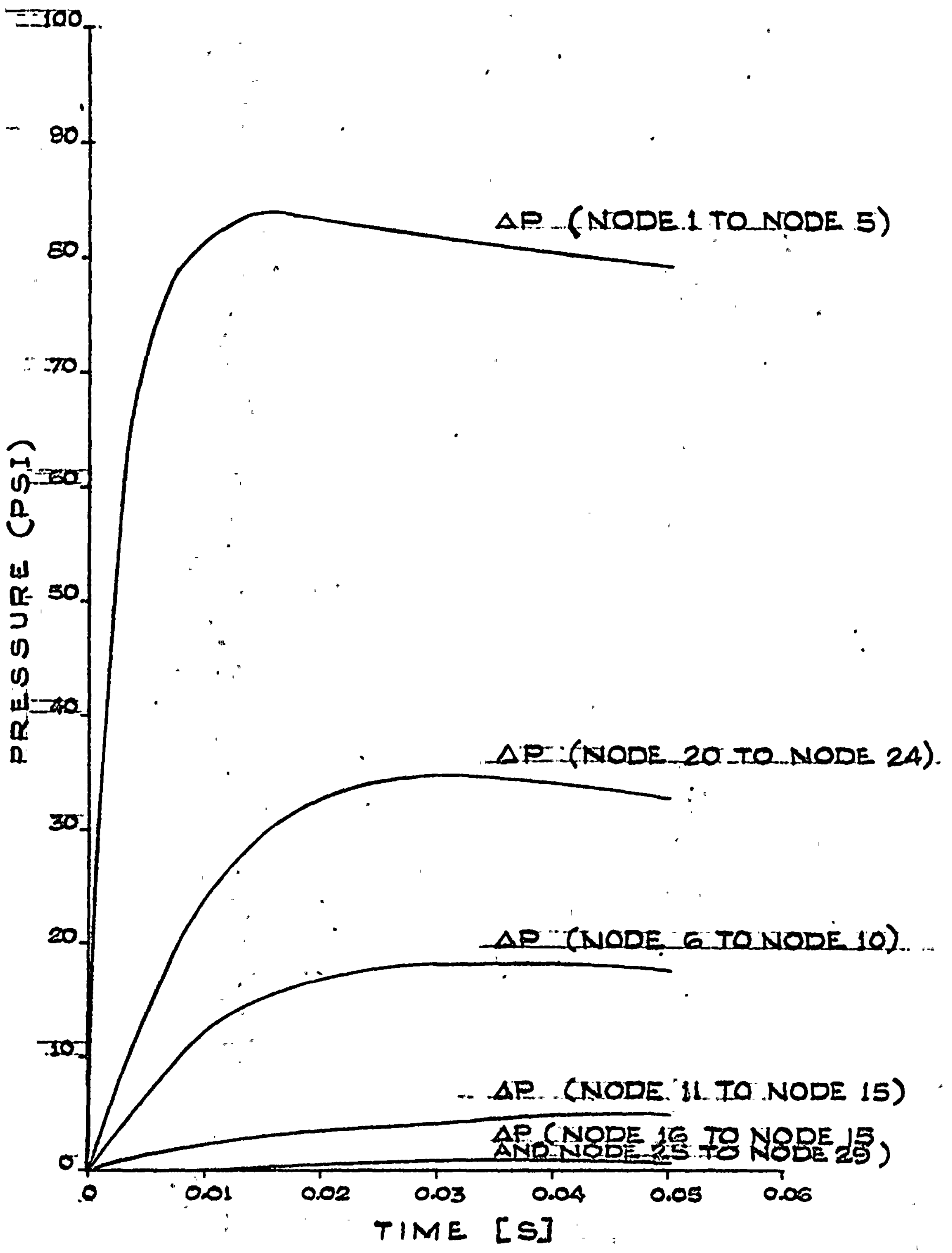

WASHINGTON PUBLIC POWER SUPPLY SYSTEM NUCLEAR PROJECT NO. 2	SHIELD WALL ANNULUS ΔP 60 NODE CASE, 8.6:1 FLOW SPLIT	FIGURE 22

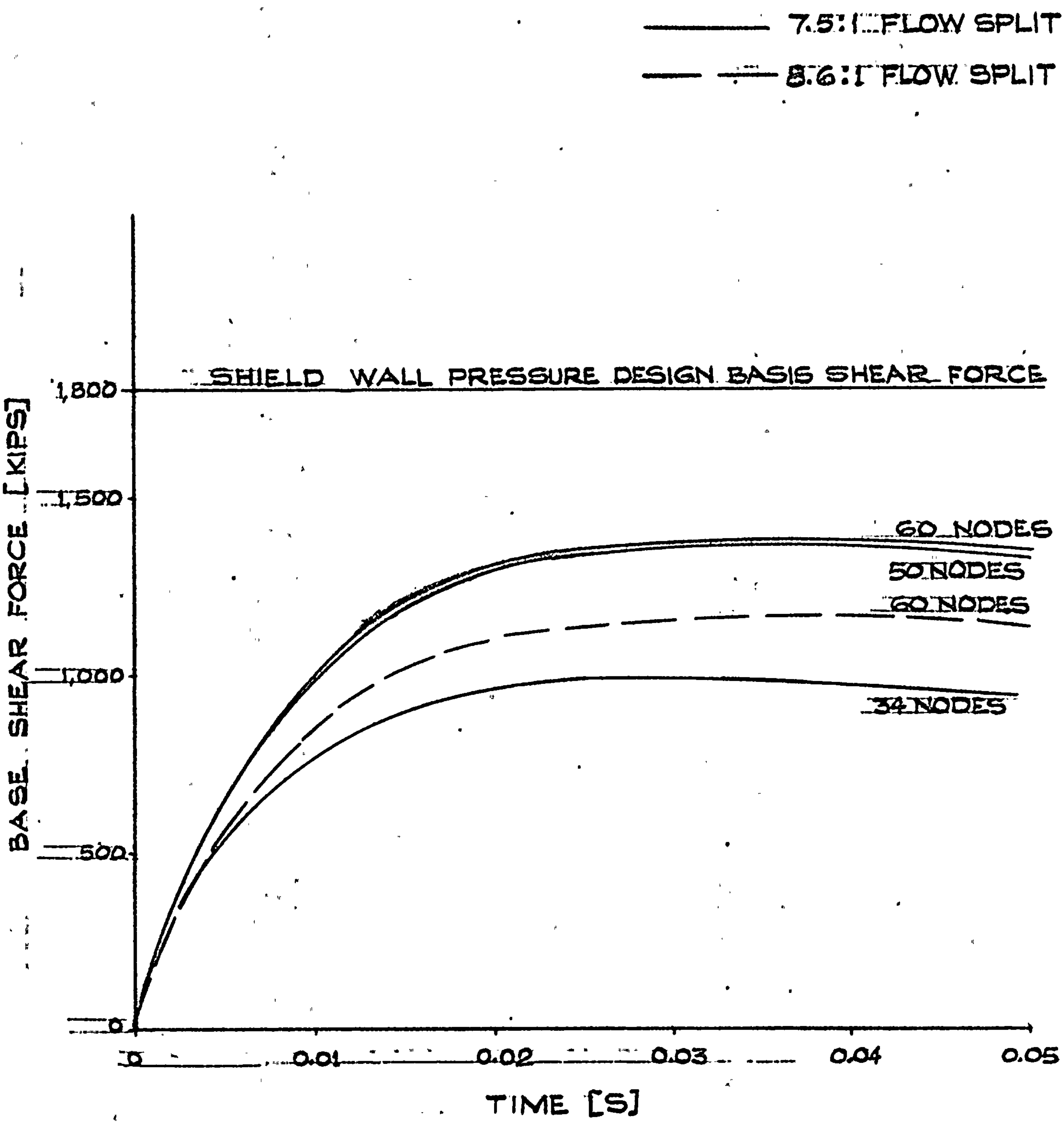

WASHINGTON PUBLIC POWER SUPPLY SYSTEM NUCLEAR PROJECT NO. 2	SHIELD WALL BASE SHEAR FORCE	FIGURE 23

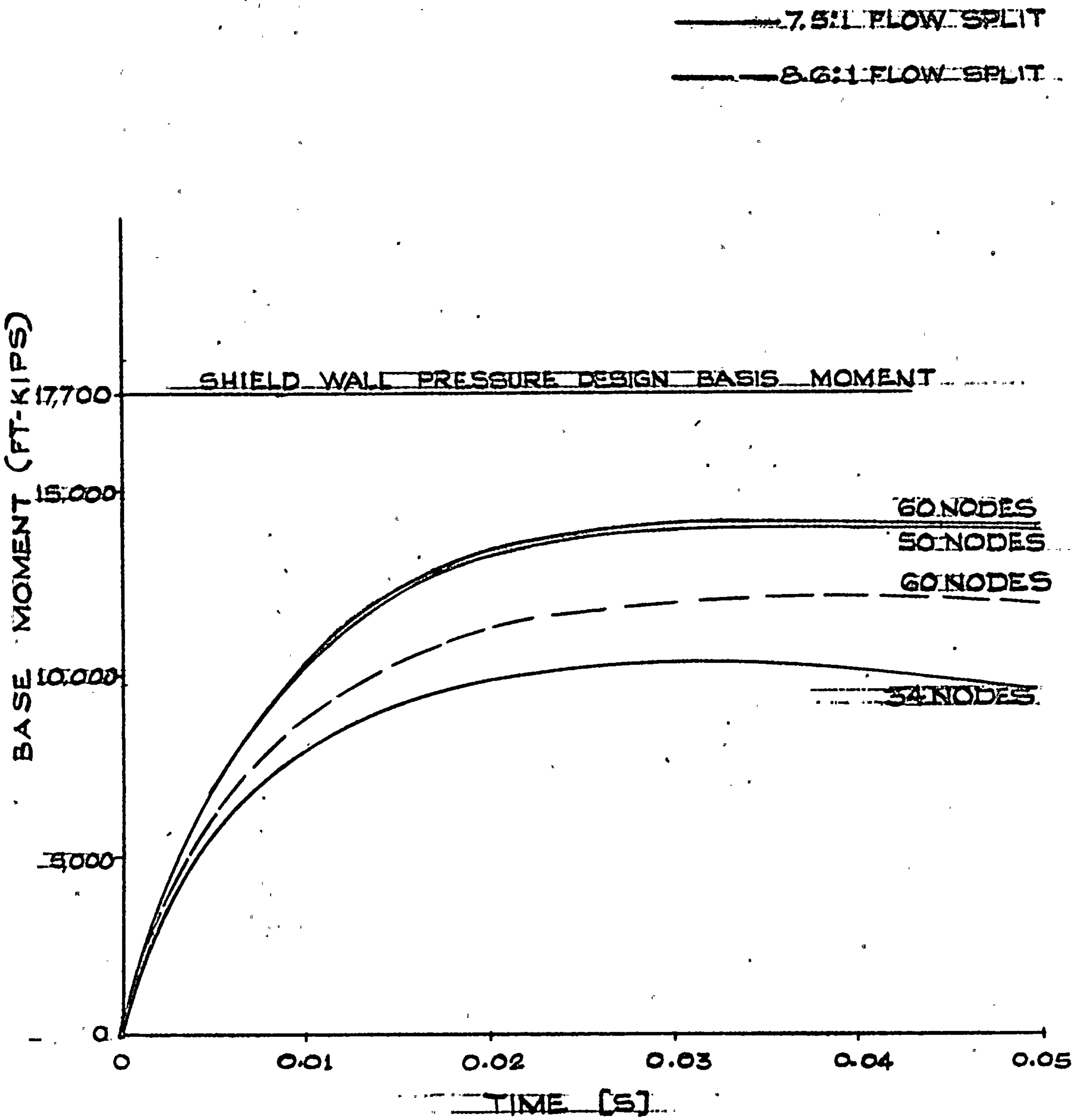

WASHINGTON PUBLIC POWER SUPPLY SYSTEM NUCLEAR PROJECT NO. 2	SHIELD WALL BASE MOMENT	FIGURE 24

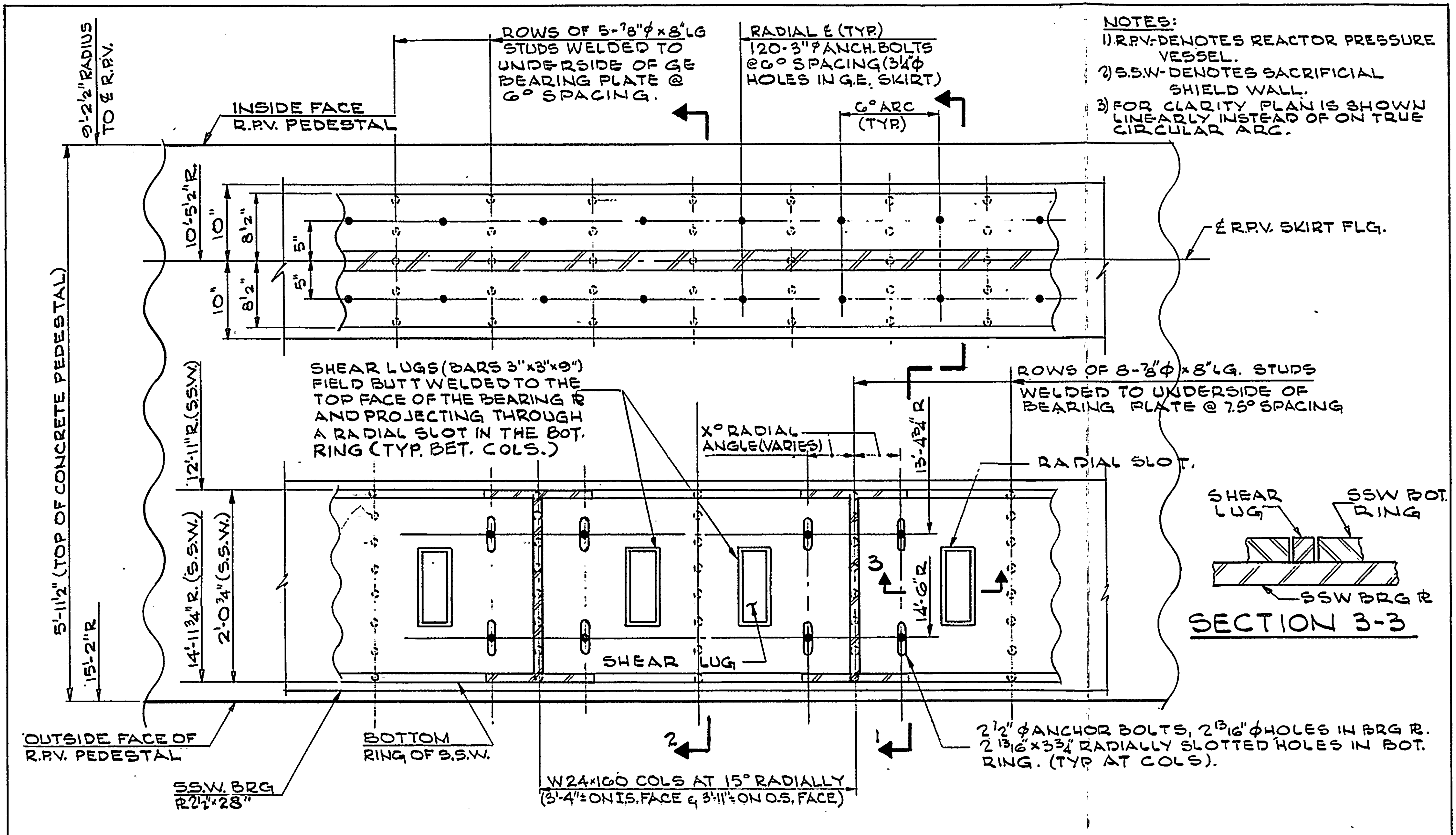

PLAN
(AT TOP OF PEDESTAL)
BASE DETAILS OF SSW & RPV.

WASHINGTON PUBLIC POWER SUPPLY SYSTEM - NUCLEAR PROJECT No. 2

FIGURE 25

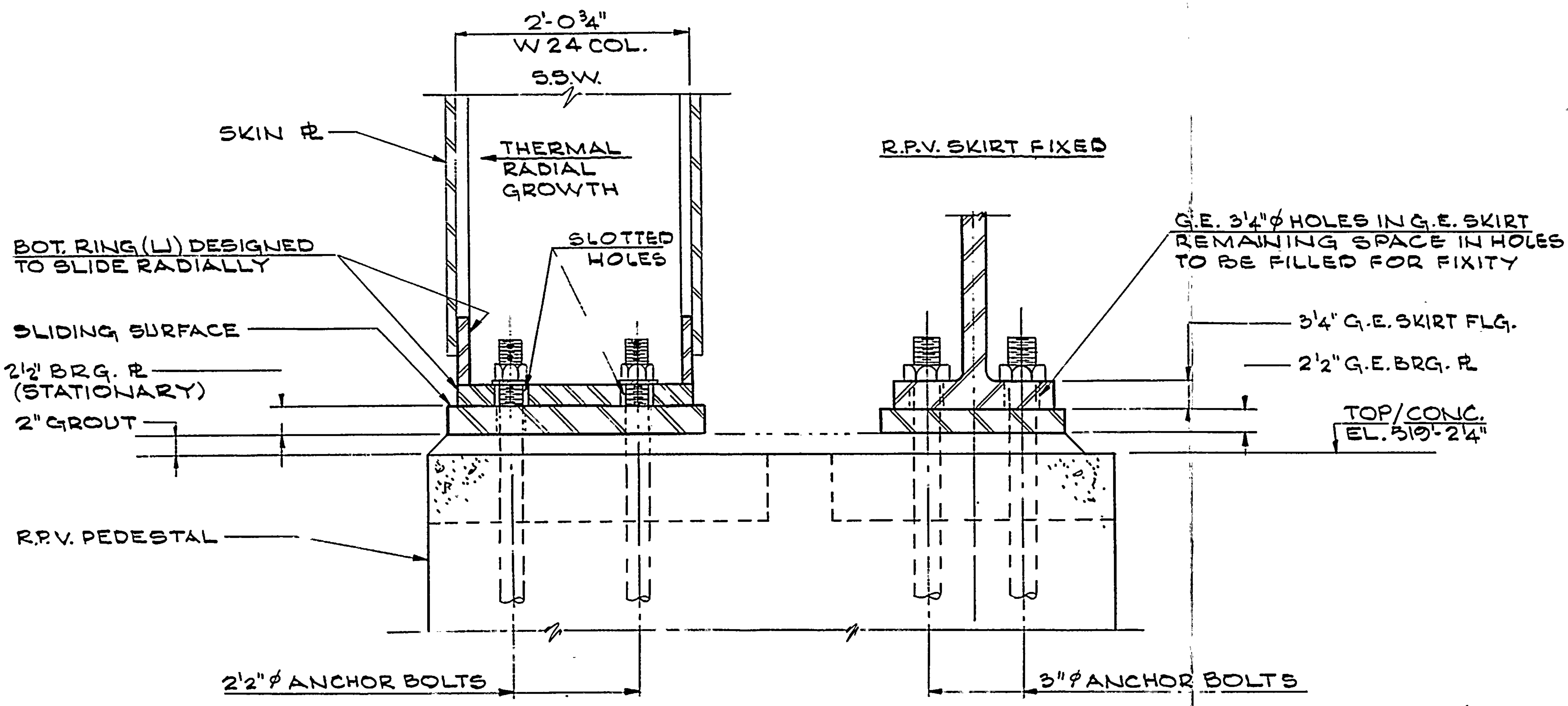

SECTION 1-1

(BASE DETAILS OF S.S.W. & R.P.V.)

SCALE 1"=1'-0"

WASHINGTON PUBLIC POWER SUPPLY SYSTEM - NUCLEAR PROJECT No. 2

FIGURE 26

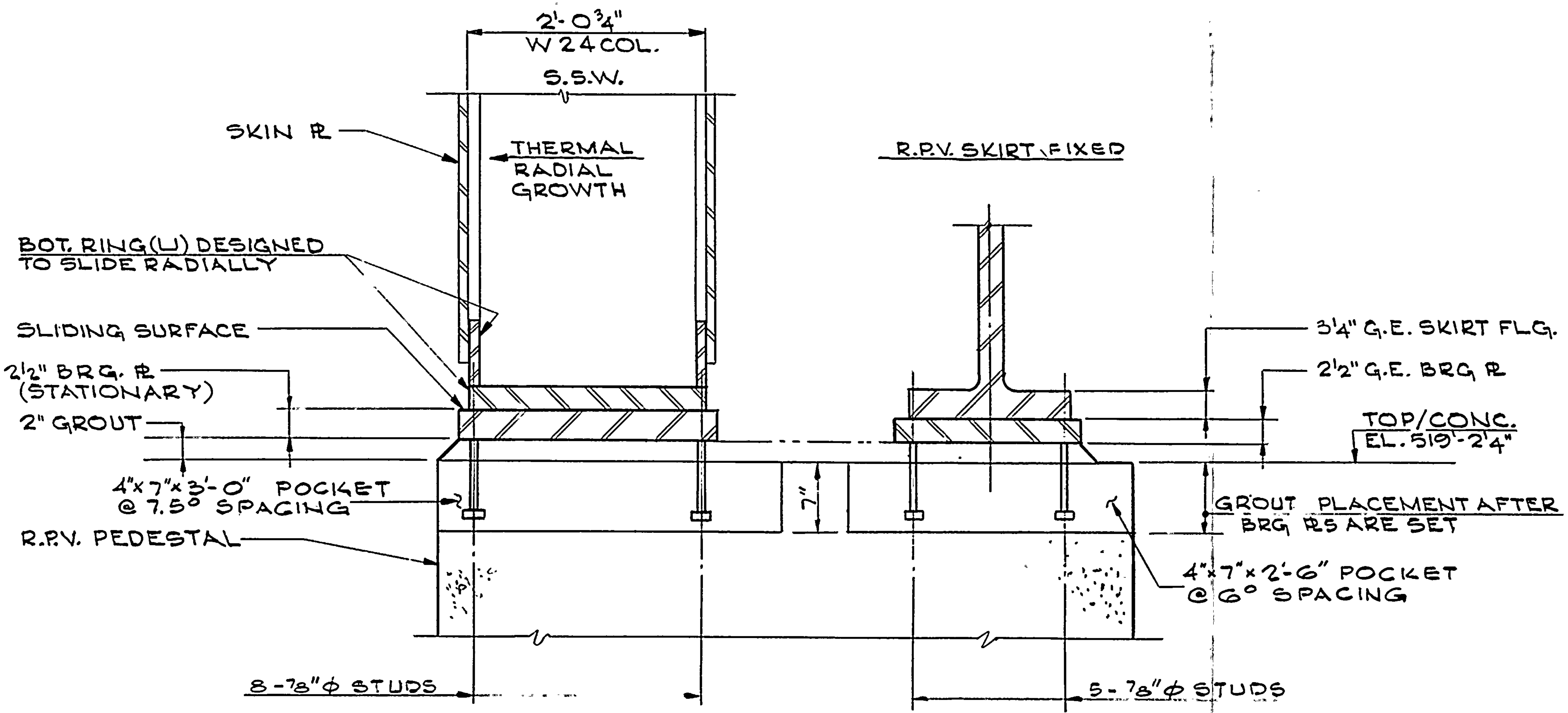

SECTION 2-2

(BASE DETAILS OF S.S.W. & R.P.V.)

SCALE 1"=1'-0"

WASHINGTON PUBLIC POWER SUPPLY SYSTEM - NUCLEAR PROJECT No. 2

FIGURE 27